NASA IN D-783

NASA TN D-783

Copy 1

TECHNICAL NOTE

D-783

A PRELIMINARY STUDY OF A SOLAR-PROBE MISSION

By Duane W. Dugan

Ames Research Center
Moffett Field, Calif.

NATIONAL AERONAUTICS AND SPACE ADMINISTRATION

WASHINGTON April 1961

NATIONAL AERONAUTICS AND SPACE ADMINISTRATION

TECHNICAL NOTE D-783

A PRELIMINARY STUDY OF A SOLAR-PROBE MISSION

By Duane W. Dugan

SUMMARY

A preliminary study is made of some problems associated with the sending of an instrumented probe close to the Sun for the purpose of gathering and telemetering back to Earth information concerning solar phenomena and circumsolar space. The problems considered are primarily those relating to heating and to launch requirements. A nonanalytic discussion of the communications problem of a solar-probe mission is presented to obtain order-of-magnitude estimates of the output and weight of an auxiliary power supply which might be required.

From the study it is believed that approaches to the Sun as close as about 4 or 5 million miles do not present insuperable difficulties insofar as heating and communications are concerned. Guidance requirements, in general, do not appear to be stringent. However, in terms of current experience, velocity requirements may be large. It is found, for example, that to achieve perihelion distances between the orbit of Mercury and the visible disc of the Sun, total burnout velocities ranging between 50,000 and 100,000 feet per second are required.

INTRODUCTION

The development of rockets powerful enough to launch sizable payloads into deep space essentially free of the Earth's gravitational attraction has opened up new opportunities for exploration of the cosmic environment. It appears logical that advantage of this opportunity will be taken to make a close-range study of the nearest star and governing body of a planetary system, the Sun.

Although the close relationship between solar activity and terrestrial phenomena, such as the polar auroras, magnetic storms, disruption of radio communication, and climate and weather, is currently recognized, the causal nature of the relationship is not completely understood, nor are the solar events themselves adequately explained or predicted on the basis of present knowledge. Enclosed as he is by a shielding magnetic field and filtering atmosphere, and separated from the Sun by 93,000,000 miles, Earth-bound man can obtain only partial information concerning the corpuscular and radiative output of the Sun, and the nature of magnetic and electric fields of circumsolar space. However, an instrumented probe can be employed to collect and telemeter back to Earth desired data over the region between the Earth and the Sun.

The purpose of the present study is to obtain an indication of the nature and severity of what appear to be major problems inherent in a solar-probe mission. A solar-probe mission is here defined as the acquisition of information relating to solar phenomena and to circumsolar space by means of an instrumented probe launched from Earth into trajectories passing within the orbit of Mercury. It is obvious that the capabilities of the instrumentation and of the communications system should be such that the accuracy and extent of the acquired data are greater than that which could be obtained from Earth or near-Earth observatories.

An analysis of the heating arising from absorption of solar radiation is made in an attempt to estimate how near a probe might approach the Sun without exceeding allowable temperatures of structure or of components of a scientific payload. The three-dimensional motion of an Earth-launched vehicle is analyzed to find the velocity requirements under optimum burnout conditions for solar orbits of given perihelion distances, and to determine effects of launching errors upon the characteristics of the orbits. Communications requirements of the solar-probe mission are pointed out, and a brief discussion is given of probable magnitudes of spaceborne powers and of power-supply weights which may, in view of current advances in the art of deep-space communications reported in the literature, meet these requirements.

TEMPERATURE CONSIDERATIONS

As indicated in the Introduction, the nearness of approach of a probe to the Sun may be limited by the temperatures which can be tolerated either by the structure of the probe itself or by the scientific payload it carries. Once in orbit about the Sun, a probe is subject to several sources of heating, namely, absorption of solar thermal radiation, solar atmospheric heating, and generation of heat by components of the payload. The temperatures sustained on a probe and its payload will be governed by the rate at which the total heat is reradiated.

Although the temperature of the visible solar corona is estimated at 1,000,000° Kelvin, this portion of the solar atmosphere is apparently so tenuous that the passage of a body through it results in inappreciable deceleration or heating (pp. 254-5 of ref. 1, pp. 241-2 of ref. 2). In addition, the visible portion of the corona generally extends only a few solar radii from the Sun (as far as 24 radii at the solar equator in extreme cases); thus, any heating of a probe from the relatively few collisions with the particles comprising the corona may appear negligible compared with that due to absorption of thermal radiation at such distances. The effect of solar flares, on the other hand, may be appreciable should a probe pass very close to the Sun. Since such contingencies cannot be predicted, and because quantitative estimates of the effects of solar flares on the temperature of a probe cannot be given, the subsequent analysis does not take solar-flare activity into account. The design of a solar probe, however, should include some margin of safety with regard to maximum temperatures.

In order to dissipate the heat generated internally by components of a payload, the temperature of the surrounding walls of a probe should be somewhat lower than the maximum temperature which can be tolerated by the payload. Inasmuch as the chief source of heating is likely to be the Sun rather than the internal heat generators, particularly when close to the Sun, attention is now turned to the estimation of the temperatures which can be expected as a result of absorption and reradiation of solar thermal radiation by the surfaces of a solar probe.

Consider the Sun a black body with a surface temperature $T_\odot$. At a distance r from the center of the Sun, the rate of heat Q_a absorbed by a body of effective absorbing area S_a is

$$Q_a = S_a T_\odot^4 (r_\odot/r)^2 \alpha\sigma \tag{1}$$

where α is the absorptivity with respect to solar radiation, σ is the Stefan-Boltzmann constant, and $r_\odot$ is the radius of the Sun. (A list of symbols used in this report is given in appendix A.) In general, the vehicle may have nonuniform surface temperatures and emissivities, so that the rate of heat radiation is given by

$$Q_r = \sum S_i T_i^4 \epsilon_i \sigma \tag{2}$$

where ϵ_i is the emissivity of each surface S_i having the uniform temperature T_i. The sum of the individual surfaces involved in radiating heat is, of course, the total surface area.

As a first example, assume a probe has a spherical shape, and assume further that the temperature is essentially uniform over the surface by reason of rotation and/or high heat conductivity. It follows that the equilibrium temperature T_E at a given distance from the Sun is a function only of the fourth root of the ratio of the absorptivity to the emissivity:

$$T_E = (1/2)^{1/2} (\alpha/\epsilon)^{1/4} T_\odot (r_\odot/r)^{1/2} \tag{3}$$

In general, the thermal properties of materials are temperature dependent. Data on emissivity and absorptivity (particularly the latter) at elevated temperatures for materials of interest are scanty at the present writing. In the case of good conductors (metals) the following rule, developed from electromagnetic theory, has been shown to be valid (ref. 3): The absorptivity of a metal surface at temperature T_1 with respect to radiation from a black body at temperature T_2 is equal to the emissivity at a temperature $(T_1T_2)^{1/2}$. From the handbook values for total hemispheric emissivities, and from the above rule for absorptivities with respect to solar radiation, curves of ϵ and α, and of their ratio were constructed as functions of absolute temperature for two metals of high reflectivity, silver and aluminum. These curves are presented in figure 1 to illustrate the change of thermal properties over a wide range of temperatures for metals. Clearly the ratio α/ϵ decreases with increasing temperature, thereby tending to reduce the variation of temperature with distance from the Sun.

If the ratio α/ϵ were independent of temperature, the equilibrium temperatures of a spherical probe with uniform surface temperature would vary with the distance from the Sun, as shown in figure 2. Such variation can be used to determine the variation of equilibrium temperature with distance from the Sun in the case of materials with temperature-dependent thermal properties. For a given equilibrium temperature, the ratio of the absorptivity to the emissivity can be found from results such as those in figure 1. With this value of the ratio, the distance from the Sun at which the selected temperature would obtain can be found from figure 2. The variation of equilibrium temperature derived in the manner described is given in figure 3 for the case of silver and aluminum spheres. It can be seen from figure 2 that even with fractional values of α/ϵ as small as 0.5, a spherical probe of uniform surface temperature could not approach the Sun more closely than approximately 0.6 of an astronomical unit without exposing the payload to temperatures above 600° R. Solar orbits having perihelion distances no smaller than the above figure would not be particularly interesting or useful from the standpoint of the present mission.

Next consider a spherical probe oriented so that one hemisphere is in perpetual sunlight and the other in perpetual shade. (Actually, of course, slightly more than one-half of the total surface will be sunlit, depending upon how close the probe approaches the Sun; for the present purpose it is sufficient to consider that the exposed and shaded areas are equal.) The temperatures over the surface will then depend upon the rate of heat flow by radiation and conduction from the heated surfaces to the shaded areas. At one extreme the rate of heat transmission might be considered great enough to maintain the unexposed areas at the same uniform temperature as that of the absorbing surfaces; thus the situation would be identical to the one in the first example. At another extreme, the two hemispheres could be completely thermally isolated (in theory). In this case the temperature of the sunlit hemisphere would be $(2)^{1/4}$ times or nearly 19 percent greater than the temperature given by equation (3), whereas the temperature of the other half of the sphere would reach nearly absolute zero. Regulation of the heat transmitted from the heated surfaces to the shaded surfaces could maintain a region within the probe at temperatures compatible with the requirements of the payload. The regulation of the heat transferred by radiation might be accomplished by employing highly reflective shields to retard the radiant heat flow to the interior, or to reduce the loss of heat to shaded surfaces. The temperature of the walls of the hemisphere unexposed to solar radiation could be controlled by varying the area available for thermal conduction between the two hemispheres, and perhaps by also varying the emissivity characteristics of the shaded surfaces. By confining the high temperatures to the sunward portions of the probe structure, approaches closer to the Sun are possible compared with the figure cited for the first example.

Higher ratios of radiating surface to absorbing surface than is possible in a sphere are provided by a configuration consisting of a hemisphere followed by a right conical frustum. The longitudinal axis of the probe would be constantly pointed toward the Sun. The apex angle of the conical frustum would be determined by the condition that no sunlight reach its surface at the nearest approach to the Sun. The semiapex angle is equal to $\sin^{-1}(r_\odot/r)$; thus, even at distances as small as 10 solar radii (less than 5,000,000 miles) from the Sun, the cone angle would be less than 12°. A simplified analysis of the temperature distribution which results from solar heating is made here for the configuration described to determine the effect of the several thermal properties upon the temperatures of the sunlit and of the shaded areas.

A number of assumptions are made to simplify the analysis. To begin with, the configuration is taken as a hollow cylinder of length L and radius ρ with a hemisphere of the same radius at one end, oriented with respect to parallel solar radiation as shown in sketch (a). It is assumed

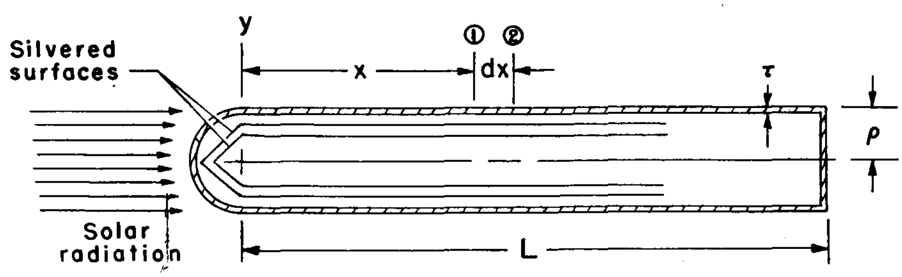

Sketch (a)

that a sufficient number of closely spaced reflective shields inside the hemisphere and extending for some distance along the cylinder perform two functions: first, in conjunction with the conductivity of the hemispherical shell, the shields decrease the temperature gradient over the hemisphere to nearly zero so that the assumption of uniform temperature on this portion of the probe is valid; secondly, the shields can reduce the transfer of radiant heat rearward to amounts small compared with that transmitted by conduction of the outer shell of the probe structure. The thickness τ of the cylindrical walls will be small in comparison with the radius ρ in order to keep the weight low, so that the cross-sectional area of the shell may be approximated by $2\pi\rho\tau$ without serious error. Furthermore, the heat radiated from the base of the cylinder is regarded as negligible compared to that radiated by the cylinder walls; this assumption implies that the length of the cylinder is several times the radius. Other simplifications will be made as the analysis proceeds in order to avoid unwieldy expressions, although not at the expense of losing sight of the basic principles it is intended to illustrate.

Under the above assumptions, the rate of heat Q_1 entering the volume element $2\pi\rho\tau\ dx$ from the left (sketch (a)) is

$$Q_1 = -2\pi\rho k\tau \frac{dT}{dx} \tag{4}$$

The thermal conductivity k of the shell is considered here to be constant at an effective value over the range of temperatures from one end of the cylinder to the other; from another viewpoint, the product $k\tau$ can be considered to be constant, so that the variation in thickness of the shell compensates for the change in conductivity with temperature. Next, the rate of heat leaving the elemental volume by radiation to space is

$$dQ_r = \epsilon_w\sigma(2\pi\rho\ dx)T^4 \tag{5}$$

where ϵ_w is the effective value of the emissivity of the wall surface. The flow of heat leaving the same elemental volume by conduction is

$$Q_2 = -2\pi\rho k\tau\left[\left(\frac{dT}{dx}\right) + \left(\frac{d^2T}{dx^2}\right)dx\right] \tag{6}$$

Under steady conditions, the heat flow given by equation (4) is equal to the sum of those given by equations (5) and (6), so that

$$\frac{d^2T}{dx^2} = \frac{\epsilon_w\sigma}{k\tau}\,T^4 \tag{7}$$

A first integration of equation (7) gives

$$\left(\frac{dT}{dx}\right)^2 = \frac{2}{5}\,\frac{\epsilon_w\sigma}{k\tau}\,T^5 \tag{8}$$

where the constant of integration is taken to be zero, since when T approaches zero, so does the temperature gradient dT/dx. Implied in the boundary condition is a cylinder of infinite length. However, in view of the magnitude of the exponent associated with the variable T, the above equation should be a good approximation in the case of cylinders whose length is several times greater than the radius. The solution of equation (8) is

$$T = (Cx + T_o^{-3/2})^{-2/3} \tag{9}$$

where T_o is the absolute temperature at $x = 0$, and $C^2 = 0.9(\epsilon_W\sigma/k\tau)$.

A heat balance between the heat absorbed and reradiated by the probe will now be determined. Recall that the temperature of the hemisphere was assumed uniform. The uniform temperature is, of course, T_o. From equation (2) the rate of heat radiated by the probe is

$$Q_r = 2\pi\rho^2\epsilon_1\sigma T_o^4 + 2\pi\rho\epsilon_W\sigma\int_0^L T^4 dx$$

where ϵ_1 is the emissivity of the hemisphere. Integration of this equation, with T given by equation (9), yields

$$Q_r = 2\pi\rho^2\sigma\left[\epsilon_1 T_o^4 + \frac{3}{5}\frac{\epsilon_W}{\rho C}(T_o^{5/2} - T_L^{5/2})\right] \tag{10}$$

where T_L is the value of T at $x = L$. Under conditions of equilibrium,

$$Q_a = \pi\rho^2\alpha\sigma\left(\frac{r_\odot}{r}\right)^2 T_\odot^4 = Q_r = 2\pi\rho^2\sigma\left[\epsilon_1 T_o^4 + \frac{3}{5}\frac{\epsilon_W}{\rho C}(T_o^{5/2} - T_L^{5/2})\right] \tag{11}$$

Solving for the distance r, we obtain

$$\bar{r} = \frac{r}{a} = \frac{(1/2)^{1/2}(\alpha/\epsilon_1)^{1/2}T_\odot^2(r_\odot/a)}{T_o^2\sqrt{1+0.6(\epsilon_W/\epsilon_1)(1/\rho C)(1/T_o^{3/2})\left[1-(T_L/T_o)^{5/2}\right]}} \tag{12}$$

where a is the astronomical unit, the semimajor axis of the orbit of the Earth. It can be seen that to minimize $\bar{r}$ for a given T_o, both α and ϵ_1 should be as small as possible relative to ϵ_W. Equation (12) is plotted in figure 4 for a configuration with a silver hemisphere followed by a cylindrical section of material having various values of "effective conduction" $k\tau$, of emissivity ϵ_W, and having radius ρ and length L. (A value of unity for $k\tau$ would be represented, for example, by an aluminum-copper alloy about 1/8 inch thick.) Figure 5 shows the variation of temperature along the cylinder walls for different values of T_o and for the same parameters $k\tau$ and ϵ_W used in figure 4. It is to be noted that wall temperatures a few feet from the forward end of the cylinder differ comparatively little, regardless of the wide range of temperatures T_o of the hemisphere. The results presented in figures 4 and 5 are not to be regarded as definitive; they merely illustrate the possibilities of achieving adequate wall temperatures for temperature control of the scientific payload by varying the thermal properties of a probe structure and the dimensions of a probe configuration. To obtain adequate temperatures over a probe for the least weight of probe structure and of reflecting shields calls for more exact analysis and some experimentation. The power dissipated internally by the telemetry and possibly other equipment of the scientific payload must be known in addition to the least distance the probe is expected to approach the Sun.

From the foregoing analysis of the heating problem of a solar probe, it is believed that by proper selection of materials and dimensions, an instrumented probe can be designed to orbit as close to the Sun as 0.05 A.U. insofar as temperature considerations are concerned, provided the rate of heat generated internally by power-consuming components of a payload is small relative to the rate of heat absorbed from the Sun. At a distance of 0.05 A.U., the latter rate amounts to about 1400 Btu/min, or 25 kilowatts for a probe with a silver hemisphere at a temperature T_o of 2000° R, and with a radius of 1 foot. In a subsequent section, an order-of-magnitude estimate of the auxiliary-power requirements of a solar-probe mission indicates that they may be no more than a few hundred watts at the most.

CONSIDERATIONS OF SOLAR RADIATION PRESSURE

Before turning to an analysis of solar-probe trajectories, it is pertinent to examine the magnitude of the effects of solar radiation pressure on solar orbits of bodies as compared with those of the solar gravitational attraction in order to decide whether solar radiation pressure should be considered in the derivation of the equations of motion for a solar probe.

As shown in appendix B, the ratio of the radial acceleration resulting from the pressure of solar radiation to that caused by the solar gravitation depends only upon the weight and surface area of the body, according to the equation

$$a_r/g_\odot = -156(W/S_f')^{-1}\times 10^{-6} \tag{13}$$

where S_f' is defined as an effective frontal area which takes into account such factors as shape, orientation with respect to solar radiation, and surface characteristics of the body.

Equation (13) is plotted in figure 6; also shown in the figure are the ratios of weight to effective frontal area for several representative space vehicles, including instrumented probes and light-weight balloons. For values of W/S_f' typical of instrumented probes, figure 6 indicates that the force due to radiation pressure is of the order of 10^{-3} percent of the gravitational attraction. Since the magnitude of the latter is not known to any greater accuracy than the figure cited, inclusion of effects of solar radiation pressure in an analysis of the trajectory of an instrumented solar probe does not appear warranted in the present study.

Inasmuch as several proposals for utilizing solar radiation pressure as a means of propulsion for space vehicles have been made in recent years (see, e.g., ref. 4), it appears pertinent to examine such proposals here, particularly with regard to their applicability to a solar-probe mission.

Briefly, the assumptions underlying the above proposals are these: By employing a sufficiently large area of extremely thin, light-weight plastic film on which a minimum thickness of aluminum is deposited to make the sail reflective (about 300 Å are required for adequate opacity), a ratio of area to combined weight of sail and vehicle can be obtained to make the acceleration due to radiation pressure a sizable fraction of that due to solar gravitation. The sail is assumed to be 100 percent specularly reflective so that the pressure is a maximum and is always normal to the sail. Thus, the direction of the thrust due to radiation pressure can be varied by changing the orientation of the sail with respect to the radiation. However, the area of sail required in practice would be large. For example, about 5 acres of sail would be required to impart a maximum radial acceleration equal to 1/2 that of the gravitational acceleration of the Sun in the case of a vehicle weighing, without sail, 100 pounds. Also, at the optimum orientation of the sail, the radial component of thrust is $\sqrt{2}$ times as large as the component normal to the radius vector, and the latter is less than 40 percent of the maximum available thrust. The radial component would reduce the effectiveness of solar sailing in an application to a solar-probe mission. The additional weight of equipment required to manage the sail would further degrade effectiveness. Furthermore, it is estimated in reference 5 that under "quiet" solar conditions at the Earth's distance from the Sun but beyond the protective influence of the terrestrial magnetic field, an aluminum coating 300 Å thick would be completely stripped from the plastic film of a solar sail by sputtering within one month of exposure to the solar plasma. The statement is also made that a single encounter with a solar flare could conceivably destroy the reflective coating. Increasing the thickness of the aluminum coating would probably not be the answer, since the specular reflectivity of the surface would likely be lost shortly after exposure, with a resultant serious degradation of sail efficiency. It can be demonstrated that the loss of regular reflective properties would make the solar sail an unattractive means of propulsion for a solar-probe mission. In view of the uncertainties associated with the feasibility of solar sailing at the present writing, solar radiation pressure is not considered a means of propulsion in the present study.

TRAJECTORY STUDIES

A preliminary study is made here of the three-dimensional motion of a body launched into a hyperbolic orbit from the Earth in such a direction that it achieves an orbit of least perihelion distance about the Sun. Only two central forces are included in this exploratory study, namely, those of the Earth and the Sun. Solutions to the restricted three-body problem are obtained numerically by an IBM 704 high-speed digital computer. In order to gain an insight into the problem and to facilitate the machine solution, an analytic study is first made.

Analytic Study

The analytic solution is based on a simple patching of the initial geocentric hyperbolic orbit with the heliocentric elliptic orbit. Well-known two-body solutions are utilized to calculate the necessary elements of the conic trajectories.

The first step is to make a choice of the distance from the Earth at which transition from the Earth-centered orbit to the Sun-centered one might occur. To do this, consider the variation with distance of three quantities. One is the velocity of a body launched from the Earth; another is the direction of motion of the body with reference to an initial line of reference; the third is the ratio of the gravitational attractions of the Earth and Sun. Sketch (b) shows the path of a body launched from the Earth with an initial velocity V_L. The variation of the velocity of the vehicle with distance from the center of the Earth is given by

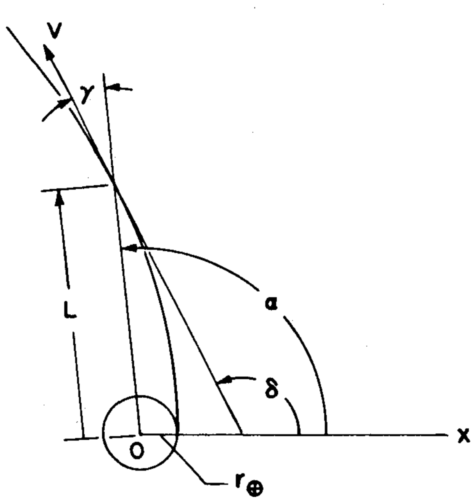

Sketch (b)

$$\tilde{V} = (\tilde{V}_L^{\,2} - 1 + \bar{L}^{-1})^{1/2} \tag{14}$$

The angle δ which defines the direction of the velocity with reference to the OX axis is the sum of the true anomaly α and the flight-path angle γ. Thus

$$\delta = \alpha + \gamma = \alpha + \cot^{-1}\left[(e\bar{L}/2\tilde{V}_L^{\,2})\sin\alpha\right] \tag{15}$$

Symbols over the quantities signify that velocities are in terms of the velocity of escape from the surface of the Earth and distances are in terms of the radius of the Earth. Figures 7 and 8 present graphical representations of equations (14) and (15), respectively. The variation of the third quantity with distance from the Earth, the ratio of the gravitational accelerations, Earth to Sun, is presented in figure 9. The expression for the ratio,

$$g_{\oplus}/g_{\odot} = 1656\ \bar{L}^{-2}$$

was derived on the assumption that the gravitational attraction of the Sun at the position of the vehicle would not differ essentially from its value at 1 A.U.

From an inspection of figures 7 and 8, it is evident that for launch velocities more than a few percent greater than escape velocity, at distances of only 30 to 50 Earth radii, the residual velocities are nearly constant in both magnitude and direction, and, furthermore, differ little from the asymptotic values. Figure 9 shows that the force of attraction of the Earth has decreased to that of the Sun on the vehicle when the latter reaches a distance of very nearly 40 Earth radii from the Earth. On the basis of the foregoing, it is concluded that transition from the geocentric orbit to the heliocentric orbit is likely to occur when the vehicle has reached a distance of between 30 and 50 Earth radii from the Earth, depending upon the velocity at burnout. To simplify the analysis somewhat, the transition point is assumed to be 40 Earth radii, regardless of the burnout velocity.

If the orbit of the Earth is assumed to be circular, it is obvious that for an Earth-launched vehicle to reach either a greatest aphelion or a least perihelion distance, the velocity of the vehicle with respect to the Earth should, at the point of transition, be collinear with the velocity of the Earth with respect to the Sun. The direction of the burnout velocity required to meet the above criterion is determined in appendix C where expressions for the initial values of the geocentric hyperbolic orbit are derived.

The sense of the direction of the residual velocity of the Earth-launched probe may, of course, be either the same as or opposite to that of the orbital velocity of the Earth. In the former case, the probe would recede from the Sun, so that a second impulse would be required (e.g., at the aphelion of the probe's orbit) in order that a close approach to the Sun would be realized. In the second case, the initial impulse would accomplish the desired objective. The two methods of attaining solar orbits of a given perihelion distance are illustrated in sketch (c). As pointed out in reference 6, it is possible in some instances to achieve a closer approach to the Sun by the two-impulse method than by the single-impulse technique for the same total imparted velocity. However, there is added complexity and greater time required for the mission when the two-impulse method is used. Requirements for achieving orbits of various perihelion distances by applying one and two velocity increments are calculated here in order to assess the several

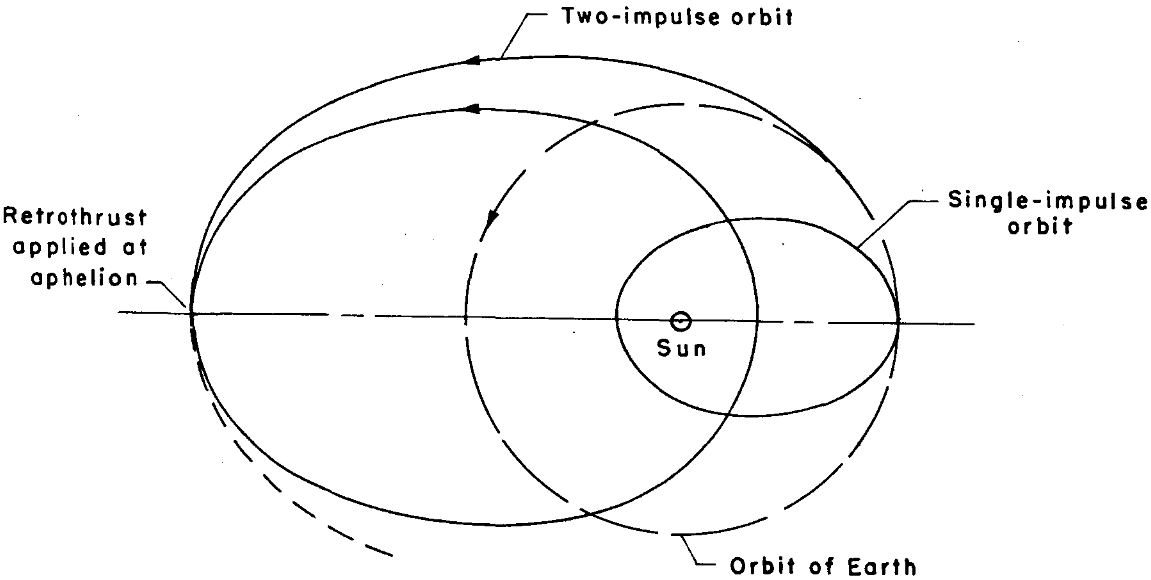

Sketch (c)

factors involved. For simplicity, the orbits are assumed to lie in the plane of the ecliptic. The most opportune time for launching in each method was taken; that is, a winter launching (Earth at perihelion) for two impulses, and a summer launching (Earth at aphelion) in the single-impulse case. The least possible perihelion distance for a given total imparted velocity is thus obtained in each method.

Figure 10 shows the relationship between the total imparted velocities and the perihelion distances obtained in the two methods. As implied in the figure, the perihelion distance achieved in the two-impulse case depends upon both the aphelion distance and the velocity imparted there. At some values of total velocity, the closest approach to the Sun is the same for both methods. The aphelion distances required to obtain the same perihelion distance as in the single-impulse method for the same total imparted velocity are shown in figure 11. The times required to reach aphelion and the times to reach perihelion in both methods are also given in the figure. It can be seen that the two-impulse method offers no velocity advantage for perihelion distances greater than about 0.22 A.U.

From the results of the above analysis, it is concluded that the single-impulse method is the more practical, except possibly for perihelion distances approaching the disc of the sun. A number of reasons may be cited. The reliability of the mission in the two-impulse method would be less than that in the case of a single impulse because of the reliance on the proper functioning of the retrorocket at the correct distance and time to change the velocity at aphelion by the necessary amount. The possibility of failure of the mission through damage from meteors is enhanced both by the greater length of time of exposure and by the more extensive distances traversed. Problems associated with temperature control and with communications would be aggravated by the large excursions beyond the orbit of the Earth that are required for the two-impulse method to be advantageous. The considerable lapse of time from launch before it would be known whether a solar orbit were achieved, or that pertinent data near the Sun would be obtained, is another factor to be considered. For example, the required operational lifetimes of some components of a payload would be excessively long by current standards.

In view of the foregoing, subsequent study of solar-probe trajectories in the present paper is confined to those obtained when the probe is launched in a direction opposite to the orbital motion of the Earth.

Numerical Study

Before presenting the results of the numerical study of solar trajectories, a brief description of the procedures used to obtain numerical solutions of the equations of motion is given here.

The equations of motion for the restricted three-body problem considered here were first developed in an inertial frame of reference. The origin was then translated alternatively to the center of the Earth and to the center of the Sun. Both geocentric and heliocentric coordinate systems were required in order to avoid computational difficulties associated with small differences of large quantities. It was found to be expedient to use the heliocentric frame of reference for Earth-probe distances larger than 0.03 A.U.

An IBM 704 high-speed digital computer was employed to obtain solutions of the equations of motion by direct numerical integration. The Adams-Moulton predictor-corrector method using the Runge-Kutta-Blum routine to start the process was employed. A truncation-error limitation of 1×10^{-8} was found to be satisfactory for the present study.

The motion of the Earth about the Sun, or vice versa, was assumed to be that of an elliptic orbit of constant eccentricity $e_\oplus$, and of sidereal period $T_\oplus$. The radius vector $\bar{R}$ in A.U. was calculated from

$$\bar{R} = (1 - e_\oplus{}^2)/(1 + e_\oplus \cos \psi)$$

where ψ, the true anomaly is calculated from

$$\psi = \int \dot{\psi}\, dt$$

The instantaneous angular rate $\dot{\psi}$ is given by

$$\dot{\psi} = n_{\oplus}(1 + e_{\oplus}\cos\,\psi)^2/(1 - e_{\oplus}{}^2)^{3/2}$$

where $n_{\oplus}$ is the mean motion (average angular velocity) of the Earth.

The numerical and analytical studies were applied to the case of a solar probe launched into a hyperbolic orbit with respect to the Earth from a burnout altitude of nearly 200 miles above the surface of the Earth and a burnout latitude corresponding to the latitude of Cape Canaveral, Florida. Two dates of launching were selected, one in early January (Earth at perihelion), the other in early July (Earth at aphelion). The burnout velocity was assumed to be tangential to the surface of the Earth. A number of solutions were obtained numerically for each of several assumed burnout velocities under the above conditions, differing only in the value of the lead angle α_2 used to determine the remaining initial conditions. Values of α_2 somewhat less than and greater than the value obtained in the analytic study were used in the machine solutions. Equations (C4) through (C9) were employed to find initial values of α, $\dot{\alpha}$, and $\dot{\phi}$.

Results

The results of both the numerical and the analytical studies are presented in the next several figures.

In figure 12, the minimum burnout velocities required at each date of launching to achieve solar trajectories having given perihelion distances are shown. An estimate of the total velocity requirements for given solar-probe missions is given in figure 13. These total velocities were calculated from the minimum burnout velocities above by assuming that the energy required to achieve burnout altitude and to overcome atmospheric drag amounted to an equivalent additional velocity of 5600 feet per second, and by taking into account the contribution of the rotation of the Earth about its axis.

The optimum time of the day at which burnout should occur to obtain the least perihelion distance for a given burnout velocity is shown as a function of burnout velocity in figure 14, and as a function of perihelion distance in figure 15. The local Sun time of the burnout point is, of course, related to the initial angle α_3 (see sketch (d), p. 27); this angle, it will be recalled, is determined from the date of launching, the latitude of the burnout point, and the value of the lead angle α_2 (cf. eqs. (C4) - (C7)).

The eccentricities and periods of the orbits defined by their perihelion distances are presented in figure 16. The eccentricity of each orbit was calculated from the Sun-probe distances at first perihelion passage and at the succeeding aphelion passage. The periods were found by doubling the time interval between the above apsides.

Figure 17 gives the aphelion distance for the corresponding perihelion distances of the solar-probe orbits. The distances of the Earth at its perihelion and aphelion are indicated also.

Under optimum burnout conditions, the angle between the line of apsides and the initial Earth-Sun axis is only a few hundredths of a degree; likewise, the angle of inclination of the solar-probe orbit is a few hundredths of a degree for the winter launching, and only a few thousandths of a degree for the summer launching. However, if burnout occurs earlier or later than the optimum time by only a few minutes, the former angle increases by about one order of magnitude, and the angles of inclination become nearly two orders of magnitude greater.

Discussion of Results

Perhaps the most noteworthy of the above results is the magnitude of the velocity requirements shown in figures 12 and 13 for various solar-probe missions. Compared with the velocity of certain currently proposed missions, such as a Martian probe or the lunar soft landing, the velocity required to send an instrumented probe within the orbit of Mercury is large. The velocity requirements rise sharply as the disc of the Sun is approached. It is also noted that they are a few percent lower for a summer launching than for a winter launching for the same perihelion distance achieved, principally because of the lower orbital velocity of the Earth at its aphelion.

From figures 14 and 15 it is seen that the optimum time for launching is slightly earlier in winter than in summer. The difference in times is due chiefly to the fact that, from a geocentric point of view, the burnout position of the probe in the present case is considerably farther out of the ecliptic plane in winter than in summer.

Figure 16 shows that the solar-probe orbits become highly eccentric as the perihelion distance approaches the radius of the Sun.

Figure 16 also shows that if no disturbances occur other than the initial perturbation by the Earth, the period of the solar-probe orbit is essentially linear with respect to the perihelion distance for the range shown. For a given perihelion distance, the period is about one week longer for summer than for winter launchings, as might be expected from the fact that Earth aphelion occurs during the summer.

From figure 17 it is noted that during its aphelion passage the probe grazes the orbit of the Earth. Furthermore, as remarked above, the lines of apsides of the probe orbits essentially coincide with the initial

Earth-Sun axis, and the orbits themselves are essentially coplanar with the plane of the ecliptic. It is clear, therefore, that barring disturbances from other bodies, it is possible that the probe will pass very near to the Earth when an inferior conjunction occurs simultaneously with an aphelion passage. The earliest possible time at which this event can take place, is, of course, one year after launch. Now, the orbit having the requisite period of one-half year is of some interest for at least two reasons. First, from figure 16, the 6-month orbit passes well within the orbit of Mercury and close enough to the Sun that any data obtained there would be of considerable value. Secondly, the total velocity required is shown in figure 13 to be only about 54,000 ft/sec. This velocity is somewhat less than that required to reach the orbit of any outer planet or to escape the solar system altogether. Another feature of the 6-month orbit is that it would offer a favorable opportunity for receiving transmission of data obtained near perihelion and stored in case unforeseen difficulties should prevent reception of the probe's signals when the probe is both at a great distance from the Earth and closest to the Sun.

Figure 18 presents the solar-probe orbit discussed in the preceding paragraph. The time chosen for launching was early January, when the Earth is at perihelion. From figures 16 and 13 it can be seen that the total velocity requirement is approximately 1500 feet per second lower for the winter than for the summer launching for this 6-month orbit. The orbits of Mercury, Venus, and Earth are also shown in figure 18. The distance between probe and Earth and the time elapsed since burnout are given at several points in the trajectory. The first half of the first revolution of the probe is given by a solid line, and the second half of the second revolution is indicated by a broken line.

In general, the effects of small errors in burnout conditions upon the characteristics of the solar-probe orbits are small, percentagewise, as illustrated in figures 19, 20, and 21. For example, from figure 19, an error of 100 feet per second in burnout velocity would change the perihelion distance by about 0.6 percent. In terms of distance, of course, the difference may represent several hundred thousands of miles. From figure 20, the same error would change the period of the orbit by only a few hours. The effect of a delay in achieving the burnout conditions prescribed for an orbit of given perihelion distance is shown in figure 21. Although the increase in the perihelion distance achieved is only a few thousand miles for delays of the order of five minutes, the effects become progressively larger for longer delays, and are considerably greater for high burnout velocities than for low. As noted earlier, other effects of a delay are the rotation of the line of apsides and the increase in the angle of inclination of the solar-probe orbit.

For a typical solar-probe mission, it is likely that the effects of any launching errors which might normally be expected on the basis of current guidance capabilities will be of little or no consequence. The actual trajectory would be determined from tracking the probe, in any case.

In the case of the orbit which is to have a close approach to the Earth one year after launch, however, the initial guidance requirements are much more stringent, depending upon the nearness of approach desired, and midcourse guidance might well be needed. Should recapture of the probe at the end of one year be contemplated for some reason, midcourse and terminal guidance would be required, not only for reasons of slight errors at launching, but also because the astronomical constants used to obtain the essential initial conditions are not known to sufficient accuracy.

Influence of Other Bodies on Solar-Probe Orbits

Inasmuch as the gravitational influence of the Moon and of other planets of the solar system on the trajectories of the Earth-launched solar probe was not taken into account in the present study, a brief discussion is given here with regard to the limitation of the results presented.

Attention is called to the generally close agreement between the results of the analytic and of the numerical studies (figs. 12-17). On the basis of such agreement, it may be concluded that the basic assumption underlying the analytic approach is nearly true; that is, that the influence of the Earth on the trajectory of the probe becomes relatively insignificant by the time the probe has receded a distance of about 40 Earth radii from the Earth. It will be recalled that the above assumption was contingent upon the fact that the relative velocity of the probe with respect to the Earth was hyperbolic. The fact that the perihelion distances found to be a minimum for a given launch velocity in the numerical restricted three-body solutions were slightly larger than those calculated by the analytic method indicates that the appreciable influence of the Earth actually extends over distances somewhat greater than 40 Earth radii. It is perhaps safe to assume that in the present circumstances, the perturbations of the solar-probe orbit by the Earth become negligible at 10 times the above distance of the probe; that is, at about 1,500,000 miles.

Because the trajectory of the probe is assumed to lie within the orbit of the Earth in the present study, the influence of the outer planets may be considered negligible without introducing appreciable error in the results obtained here.

In the consideration of the possible influences of the Moon and the two inner planets on the trajectory of the probe, several factors are taken into account. These include the masses and radii of the bodies, and the relative velocities and distances between them and the probe. Now, the nearest approach of the probe to any of the above bodies occurs when probe and body arrive simultaneously at the points where the orbit of the probe crosses (over, or under) that of the Moon, Venus, or Mercury.

It can be demonstrated that at these points the relative motion of the probe with respect to each of the planets and to the Moon is more hyperbolic than with respect to the Earth during launch.

On the basis of the above heuristic arguments, it is concluded that the results of the present restricted three-body trajectory study are valid for the present purpose, provided that a time of launching is selected so that the distances of the probe relative to the Moon, Venus, or Mercury as it crosses their orbits are sufficiently large that perturbations can be neglected.

OTHER CONSIDERATIONS

There are, of course, other considerations which need to be taken into account in planning a solar-probe mission. Some problems, such as attitude control and protection of vulnerable components against meteoroids, may be considered to be within the experience of current and past missions. Provision for considerably longer life than heretofore required will be necessary, but this does not appear to demand much more than some relatively moderate increase in weight. On the other hand, inasmuch as a solar-probe mission presents problems in communications not found in current missions, it appears pertinent to question whether it is possible to solve these problems without entailing such great power requirements and weights that such a mission becomes impractical. The chief problem, of course, is the tremendous distance over which communications need be maintained. From figure 18, which shows an orbit that in many respects is representative, the distance between the Earth and probe at perihelion of the latter is of the order of 10^8 miles. Galactic background noise, solar noise during periods near inferior conjunctions, and Doppler effects present other difficulties. Furthermore, the rate at which data would be transmitted from a probe is not likely to be only a few bits/sec, since to justify a solar-probe mission the accuracy and amount of information should be greater than that which could be obtained from near-Earth orbits. No analytic treatment of the whole communications problem is attempted here. Rather, a look is taken at the present and anticipated state of the art of deep-space communications and of auxiliary-power generation to obtain an order-of-magnitude estimate for the weight which might be required to provide the power for adequate communications in a solar-probe mission.

As is well known, considerable effort is currently being made to achieve adequate deep-space communications for future interplanetary missions. A number of facilities, devices, and techniques being developed for this purpose show promise of extending the range and usefulness of communications for space missions for modest power costs. Among these can be mentioned the construction of several large, steerable ground-based antennas; the development of a steerable spaceborne antenna of moderate gain; the design of stable oscillators of very high frequencies;

the application of masers to reduce receiver noise to very low levels; and the application of information theory to increase the amount of information which can be carried on a communication channel of given bandwidth. In reference 7, for example, it was estimated that within a four-year period, the communications system used in the lunar mission Pioneer IV could be extended to provide a two-way link over a distance as large as 4×10^9 miles with a transmitter output power of 100 watts and a receiver bandwidth of 30 cps. An Earth-seeking vehicle antenna with a 36 db gain was assumed in the foregoing estimate. If the frequency of 960.05 megacycles/sec used in the lunar mission is retained (no contemplated change was indicated in ref. 7), the diameter of this vehicle antenna can be calculated to be approximately 27 feet. For a solar probe, the antenna diameter should be no larger than that of the probe itself if provision for shielding from solar radiation is not made. There may be an optimum size for the antenna such that the ratio of the weight saved by increasing the gain to the weight of shielding required for thermal protection has a maximum greater than unity. For the present purpose, assume that the probe antenna is no more than 3 feet in diameter. A simple calculation then shows that the two-way communications system described, but with the smaller probe antenna, would require a transmitter power output of about 5 watts to have a range of 10^8 miles. If the transmitter efficiency of 7.5 percent obtained in the Pioneer IV experiment (ref. 7) were not improved in the time indicated, the required input to a vehicle transmitter would be nearly 70 watts. It is possible that the bandwidth (30 cps) would need to be increased two- or three-fold to meet requirements of a minimum information rate in a solar-probe mission. This would require greater transmitter power, two-fold for a two-fold increase in bandwidth, etc. In any case, in view of the rapidly advancing state of the art of deep-space communications, the spaceborne power requirements for communications in a solar-probe mission can be expected to be only a few hundred watts at the most within the next few years.

Because of the extended time characteristic of a solar-probe mission, some type of power converter rather than chemical batteries will likely serve as the primary source of power. The photovoltaic ("solar") cell is not well suited to a solar-probe mission. The efficiency of this device decreases with increasing temperature, and measures used to prevent high temperatures of the cells tend to decrease output or to increase weight. Other types of solar-energy converters are currently being investigated or developed. Some of these show promise of achieving attractive specific powers (watts/lb). As an example, a thermionic converter is said to have produced 7.2 watts/lb in an experimental setup, and to be capable of 17 watts/lb in the future (ref. 8). One type of thermionic converter is reported to be in commercial production, to be followed by an improved version at a later date (ref. 9). The output of the latter type may reach 20 watts per square centimeter of cathode surface, and the thermal efficiency may be as high as 30 percent, according to the reporting company. Reference 10 predicts specific weights as low as 5 lb/kw within 10 years for some solar-power converters. It thus appears that the weight of a power supply which would be required to furnish only a few hundred watts of power for a future solar-probe vehicle could be measured in tens rather than in hundreds of pounds.

CONCLUDING REMARKS

A preliminary study of a solar-probe mission has been made to obtain an indication of the nature and severity of what appear to be major problems inherent in such an undertaking. For the present purpose, the solar-probe mission was defined as the acquisition of information relating to solar phenomena and circumsolar space by means of an instrumented probe launched from Earth into trajectories passing within the orbit of Mercury. An obvious prerequisite is that the capabilities of the instrumentation and communications system be such that the accuracy and extent of the acquired data are greater than that which could be obtained from near-Earth satellites or from Earth-based observatories.

An examination of the heating problem during close approaches of a probe to the Sun indicates that perihelion distances as small as 0.05 A.U. (4.6×10^6 miles) may be feasible. The shape, dimensions, material properties, and orientation of a probe with respect to the Sun are shown to influence the maximum temperature and the temperature distribution over a vehicle at a given solar distance.

Analysis of solar trajectories obtained by launching a vehicle from the Earth indicates that the launching of the vehicle in a direction opposite to orbital motion of the Earth is generally preferable to launching in the same direction. Although for a given total expenditure of fuel it is possible, in some instances, to achieve smaller perihelion distances by launching with rather than against the orbital velocity of the Earth, there are other factors involved which will affect the choice. For one, a second impulse one or more years after launch would be required if the velocities of vehicle and Earth lay in the same direction. For another, the distance to which the vehicle would depart from the Earth in the two-impulse method would necessarily be several to many astronomical units if appreciable savings in fuel were to be realized. Likewise, the time elapsed between launch and perihelion would be measured in years in this method, rather than in months as in the single-impulse technique. Thus, any saving in fuel achieved by employing a two-impulse rather than a single-impulse trajectory is likely to be offset by a decrease in reliability, by greater hazards with respect to meteoroid damage, by aggravation of problems of temperature control and of communications, and by an objectionably long lifetime required of functioning components of a payload. Hence, in the present study, single-impulse trajectories are used in specifying trajectory characteristics of a solar probe.

To achieve perihelion distances varying between about 0.3 A.U. and the radius of the Sun, total velocities ranging between about 51,000 and

100,000 fps are required. Total velocity requirements are only approximately 2 percent less for launching at Earth aphelion (July) than at Earth perihelion (January).

Guidance requirements at launching are not stringent in terms of current capabilities. Only in the event that close approach to the Earth or recapture of a probe one year after launching were desired would mid-course or terminal guidance be necessary.

A brief discussion of the problems of communications between probe and Earth, and a look at the near-future states of the art of deep-space communications and of auxiliary-power generation, as gleaned from the literature, suggest that an adequate communications systems for a solar-probe mission could be available within a few years. Further, there is good reason to believe that spaceborne power requirements will not exceed a few hundred watts, and that the weight of the power supply may be measured in only tens of pounds in the space of a few years.

Other problems in a solar-probe mission exist, of course. Attitude control, for example, is required to maintain orientation of the longitudinal axis of a probe with respect to the Sun over periods of time measured in months. Provision for protection of vulnerable components of a payload from possible meteoroid impacts would also be essential. The combined effects of high temperatures, hard vacuums, and the solar plasma (insofar as its nature is currently known) on properties of materials should be considered in the design of a solar probe. Problems such as these are considered to be outside the scope of the present preliminary study.

Ames Research Center
National Aeronautics and Space Administration
Moffett Field, Calif., Jan. 13, 1961

APPENDIX A

NOTATION

a semimajor axis of orbit of Earth

a_r acceleration due to radiation pressure

e eccentricity of orbit

E energy

E_L azimuth angle of burnout velocity with respect to ecliptic equator (sketch (d))

F_r force due to radiation pressure

g gravitational acceleration

G Newton's gravitational constant

I inclination of solar-probe orbit to plane of ecliptic

k thermal conductivity, Btu/(hr)(ft)($^{\circ}$F)

L distance of probe from center of Earth; length of probe exclusive of nose section

$\bar{L}$ distance of probe from center of Earth in terms of Earth radii

M mass

n mean orbital motion

p_r pressure resulting from reflection or absorption of solar radiation at normal incidence

Q total rate of heat transfer

Q_a rate of absorption of thermal radiation

Q_c rate of transfer of heat by conduction

Q_r rate at which heat is radiated

r distance of probe from center of Sun

$\bar{r}$ distance of probe from center of Sun in astronomical units (A.U.)

R Rankine temperature scale

$\bar{R}$ radius vector of orbit of Earth in A.U.

S surface area

S_a surface area effective in absorbing thermal radiation

T absolute temperature; period of orbit

T_E equilibrium temperature, absolute

T_o temperature (assumed uniform) of hemispherical nose of probe

V velocity

$\tilde{V}$ $\frac{V}{V_E}$

V_E velocity of escape from surface of Earth

W weight at surface of Earth

x distance along longitudinal axis of cylindrical section of probe

α absorptivity; polar angle measured from initial Earth-Sun axis in plane of ecliptic, geocentric coordinate system

α_2 initial value of angle α at burnout, or "lead" angle in orbital plane

γ angle between probe velocity and radius vector from Earth

δ angle between probe velocity and initial Earth-Sun axis

ϵ total hemispherical emissivity

ν difference in celestial longitude of Sun and of nearest solstice (see sketch (d)); frequency of electromagnetic radiation

ρ radius of hemispherical nose or of cylindrical section of probe, ft

σ Stefan-Boltzmann constant (for black body), $Btu/(ft)^2(hr)(^{o}R)^4$

τ thickness of wall of probe structure, ft

φ polar angle of probe measured from the plane of the ecliptic in geocentric coordinate system

Subscripts

f frontal

L burnout values

$\oplus$ Earth

$\odot$ Sun

APPENDIX B

ACCELERATIONS DUE TO SOLAR RADIATION PRESSURE

Radiation pressure may be thought of as arising from the absorption or reflection of photons. The momentum of a photon is given in standard texts as $h\nu/c$, where ν is the frequency of the radiation, c is the velocity of light, and h is Planck's constant. The force dF_r due to the absorption or specular reflection of one quantum of monochromatic radiation at normal incidence is therefore

$$dF_r = d/dt(nh\nu/c)d\nu \tag{B1}$$

where n has the value of unity for absorption, and 2 for specular reflection. The integration of $h\nu$ over the entire solar spectrum of frequencies is the total energy of solar radiation, so that

$$F_r = (n/c)(dE/dt)$$

where dE/dt represents the power output of the Sun. If the Sun is considered to be a point source of radiant energy, the power density at a distance r is given by $(1/4\pi r^2)(dE/dt)$. At the mean distance of the Earth from the Sun (one astronomical unit), the average rate at which solar energy is received per unit normal area is generally accepted as 1.94 gram calories per square centimeter per minute (92.7 ft-lb per sq ft per sec). From this figure, the radiation pressure at any distance $\bar{r}$ in A.U. can be expressed as

$$p_r = 94.3n\bar{r}^{-2}\times10^{-9} \text{ lb/sq ft} \tag{B2}$$

in the case of normal incidence.

In the calculations of the forces due to radiation pressure on a body, the nature of the surface as well as the shape and orientation of the body need to be taken into account. A specularly reflecting surface at an angle θ with respect to the incident radiation experiences a force normal to the surface and of a magnitude equal to the product of the pressure given by equation (14) with n = 2, the surface area and the square of the sine of the angle θ. For black surfaces, the force is collinear with the radiation and equal to the frontal area multiplied by the pressure given in equation (14) with n = 1. If unidirectional solar radiation pressure is integrated over the surface of a sphere having either a perfectly reflecting or a totally absorbing surface, the resulting force is the same in either case, namely

$$F_r = 94.3\bar{r}^{-2}S_f\times10^{-9} \text{ lb}$$

where S_f is the frontal area $\pi\rho^2$ of the sphere. In the case of a conical shape, however, with the apex pointing toward the Sun, the force for reflecting surfaces is $2 \sin^2\alpha$ times that for absorbing surfaces, where α is the semiapex angle of the cone. The expression for the force on a body due to radiation pressure can be generalized by defining an effective frontal area S_f' so that in all cases

$$F_r = 94.3\bar{r}^{-2}S_f'\times 10^{-9}$$

Thus, S_f' will be, in general, a function of shape, orientation with respect to the solar radiation, and surface characteristics.

From the expression for the radiation force given above, and from the equation for the magnitude of the gravitational attraction of the Sun at a distance r, the ratio of the radial accelerations produced on an object subject to both forces can be expressed as

$$a_r/g_\odot = -156(W/S_f')^{-1}\times 10^{-6} \tag{B3}$$

where a_r is the radial acceleration due to absorption or reflection of solar radiation, $g_\odot$ is the solar gravitational acceleration, and W/S_f' is the ratio of the weight of the body (measured at the surface of the Earth) to the effective frontal area. Because both the radiation pressure and the gravitational attraction of the Sun have been assumed to follow the inverse-square law of distance from the Sun, the above equation applies throughout the solar system (except, perhaps, at distances so close to the Sun that convergence of the light rays should be taken into account).

APPENDIX C

DERIVATION OF INITIAL VALUES OF GEOCENTRIC HYPERBOLIC ORBIT

Sketch (d) shows the general conditions at injection of a probe into an Earth-centered hyperbolic orbit. Sketch (d) represents the northern

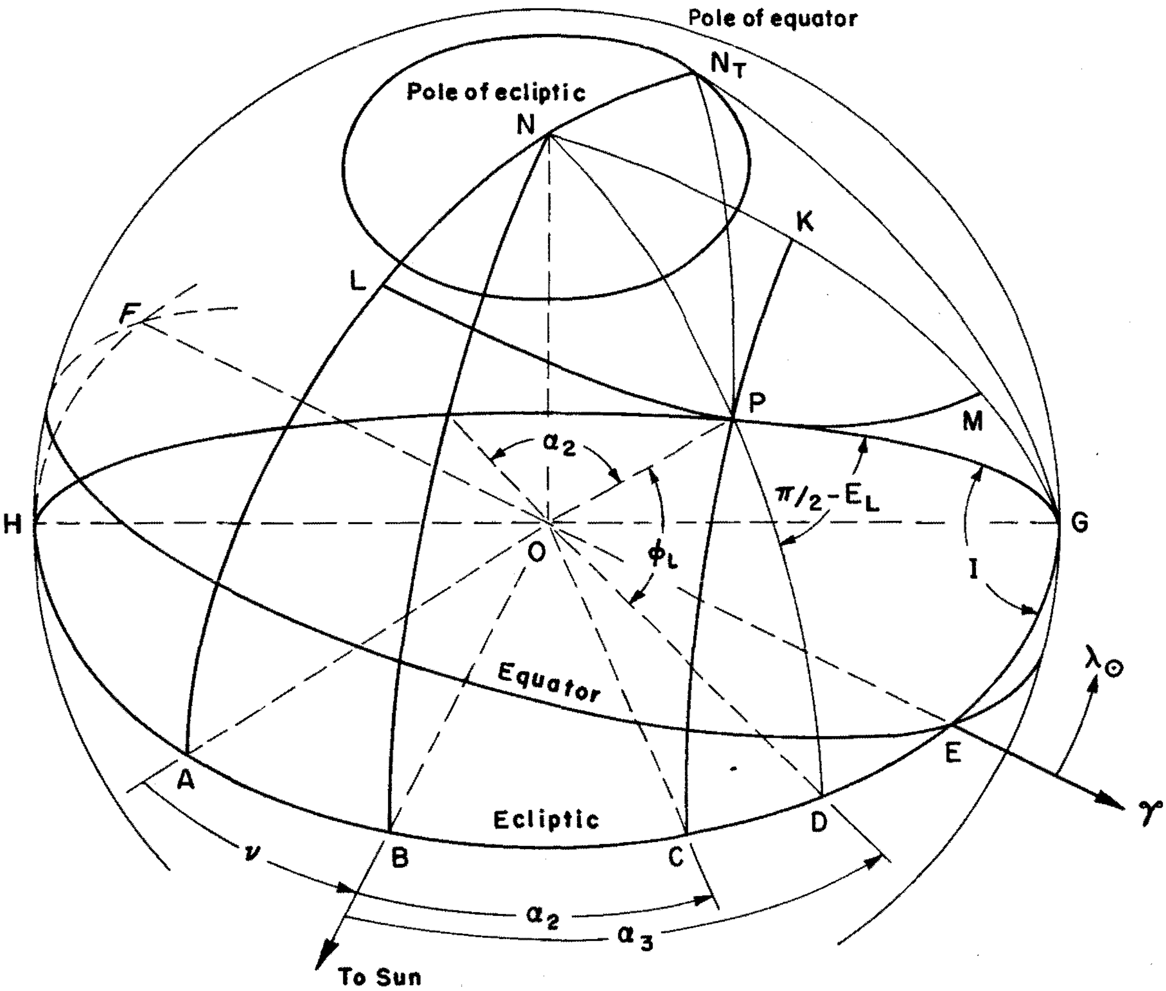

Sketch (d)

celestial hemisphere, with the Earth at its center, and with the ecliptic as the plane of reference. The initial Earth-Sun direction OB is used as a reference axis, and is given by the right ascension of the Sun $\lambda_\odot$

measured counterclockwise from the first point of Aries, γ. Point A represents the position of the Sun at the winter solstice ($\lambda_{\odot} = 270^{\circ}$); thus the initial launching conditions are shown at a time corresponding to the celestial longitude $270^{\circ} + \nu$ of the Sun. The orbital velocity of the Earth at burnout is along GOH, which may be taken without appreciable error as perpendicular to the initial Earth-Sun axis OB.

It is assumed that the burnout velocity of the probe is tangential to the surface of the Earth, and that the latitude and altitude of the burnout point are known. The position P of the probe at burnout is then located by the intersection of the two small circles LPM parallel to the equator at the given latitude from it, and CPK parallel to the meridian BN and at an angle α_2 from it. The angle α_2 is the initial or "lead" angle in the plane of the probe's orbit measured from the vertical plane BON which is required in order that the residual probe velocity will be collinear with the orbital velocity of the earth. Since the orbital equations of the probe are the same in any plane, consider the launching of the probe in the ecliptic plane as shown in sketch (e) below.

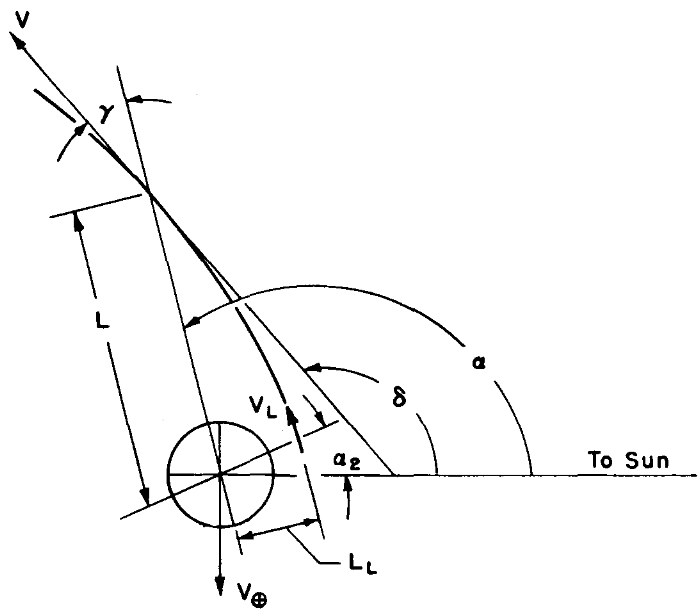

Sketch (e)

If $\tilde{V}_L$, the burnout velocity, is tangential to the Earth's surface and $\bar{L}_L$ is the initial distance from the center of the Earth, the equations of the orbit are

$$\bar{L} = 2\,\tilde{V}_L^{\,2}\bar{L}_L^{\,2}\left[1 + e\cos(\alpha - \alpha_2)\right]^{-1} \tag{C1}$$

$$e = 2\,\tilde{V}_L{}^2\bar{L}_L - 1 \tag{C2}$$

$$\gamma = \cot^{-1}\left[(e\bar{L}/2\tilde{V}_L{}^2\bar{L}_L{}^2)\sin(\alpha - \alpha_2)\right] \tag{C3}$$

If $\bar{L}$ is set equal to the assumed distance to the transition point, $\bar{L}_t = 40$, and δ is taken as $\pm 90^\circ$, the required values of the lead angle α_2 can be obtained from equations (C1), (C2), and (C3) since $\delta = \alpha + \gamma$.

With α_2 determined, the required initial angles α_3, φ_L, and E_L for given values of burnout velocity, distance from Earth, and latitude can be found as follows (provided the values of α_2 and latitude L are such that an intersection of small circles CK and LM occur):

$$\alpha_3 = \cot^{-1}(\cos I \cot \alpha_2) \tag{C4}$$

$$E_L = \tan^{-1}(\tan I \sin \alpha_2) \tag{C5}$$

$$\varphi_L = \cos^{-1}(\sin \alpha_2/\sin \alpha_3) \tag{C6}$$

The angle of inclination I which the orbit of the probe makes with the ecliptic plane is found from

$$I = \pi/2 + \cot^{-1}(\cot I_\oplus/\cos \nu) - 2\tan^{-1}(Q)^{1/2} \tag{C7}$$

$$Q = \frac{\sin(s - \pi/2 + \alpha_2)\sin\left[s - \cos^{-1}(\sin I_\oplus \sin \nu)\right]}{\sin s \sin(s - \pi/2 + L)}$$

where s is one-half the perimeter of the spherical triangle GPN_T in sketch (d). Initial values of angular velocities $\dot{\alpha}_L$ and $\dot{\varphi}_L$ are given by

$$\dot{\alpha}_L = \frac{V_L}{L_L}\frac{\cos E_L}{\cos \varphi_L} \tag{C8}$$

$$\dot{\varphi}_L = \frac{V_L}{L_L}\sin E_L \tag{C9}$$

If the values of the lead angle α_2 or of the latitude L, or of both are so great that no intersection of the two small circles occurs, the burnout velocity cannot be tangent to the surface of the Earth under the stipulated conditions. In such cases, the initial orbit becomes perpendicular to the ecliptic and to the initial Earth-Sun axis. The initial flight path angle γ_L which is required to make the residual velocity at the transition point collinear with the orbital velocity of the Earth is calculated from the same orbital equations from which α_2

was obtained. It will be found that the velocity and distance from the center of the Earth at the latitude of the burnout point will be somewhat different from those for which α_2 was determined. In the present study there was no need to apply the modified analysis to determine burnout conditions for the case of nonintersecting small circles; therefore the several necessary steps are not set forth here.

The three-dimensional characteristics of the geocentric hyperbolic orbit having been determined, the position of the probe relative to the Earth at the transition point is readily calculated from the equations of the hyperbolic orbit and of spherical trigonometry. The position of the Earth with respect to the Sun when the probe has reached the point of transition is calculated from the equation of the elliptic orbit followed by the Earth about the Sun, and from the elapsed time between burnout and arrival of the probe at the transition point. The velocity of the probe with respect to the Sun is then computed from the algebraic sum of the Earth's orbital velocity at the time of burnout and of the residual velocity of the probe at transition. The initial conditions for the elliptic orbit of the probe about the Sun then permit the calculation of all the elements of the heliocentric trajectory.

REFERENCES

1. Abetti, Giorgio: The Sun. Translated by Sidgwick, J. B., New York, Macmillan, 1957.

2. Smart, William Marshall: Celestial Mechanics. Longmans, Green and Co., Ltd., London, New York, 1953.

3. Eckert, Ernst: Introduction to the Transfer of Heat and Mass: With an Appendix on Property Values by Robert M. Drake, Jr., 1st. ed. McGraw-Hill, New York, 1950.

4. Garwin, R. L.: Solar Sailing - A Practical Method of Propulsion Within the Solar System. Jet Prop., vol. 28, no. 3, March 1958. pp. 188-190.

5. Reiffel, L.: Structural Damage and Other Effects of Solar Plasmas. ARS Journal, vol. 30, no. 3, March 1960, pp. 258-261.

6. Edelbaum, T. N.: Some Extensions of the Hohmann Transfer Maneuver. ARS Journal, vol. 29, no. 11, Nov. 1959, pp. 864-865.

7. Brockman, M. H., Buchanan, H. R., Choate, R. L., and Malling, L. R.: Extra-Terrestrial Radio Tracking and Communication. Proc. IRE, vol. 48, no. 4, April 1960, pp. 643-654.

8. Daniel, Arthur F.: Solar Batteries. Proc. IRE, vol. 48, no. 4, April 1960, pp. 636-641.

9. Anon.: Thermionic Converters Near Market. Missiles and Rockets, vol. 7, no. 10, Sept. 5, 1960, p. 15.

10. Huth, John H.: Power Supplies for Orbital and Space Vehicles. Advances in Space Science, vol. 1, Frederick I. Ordway III, ed., Academic Press, New York, 1959.

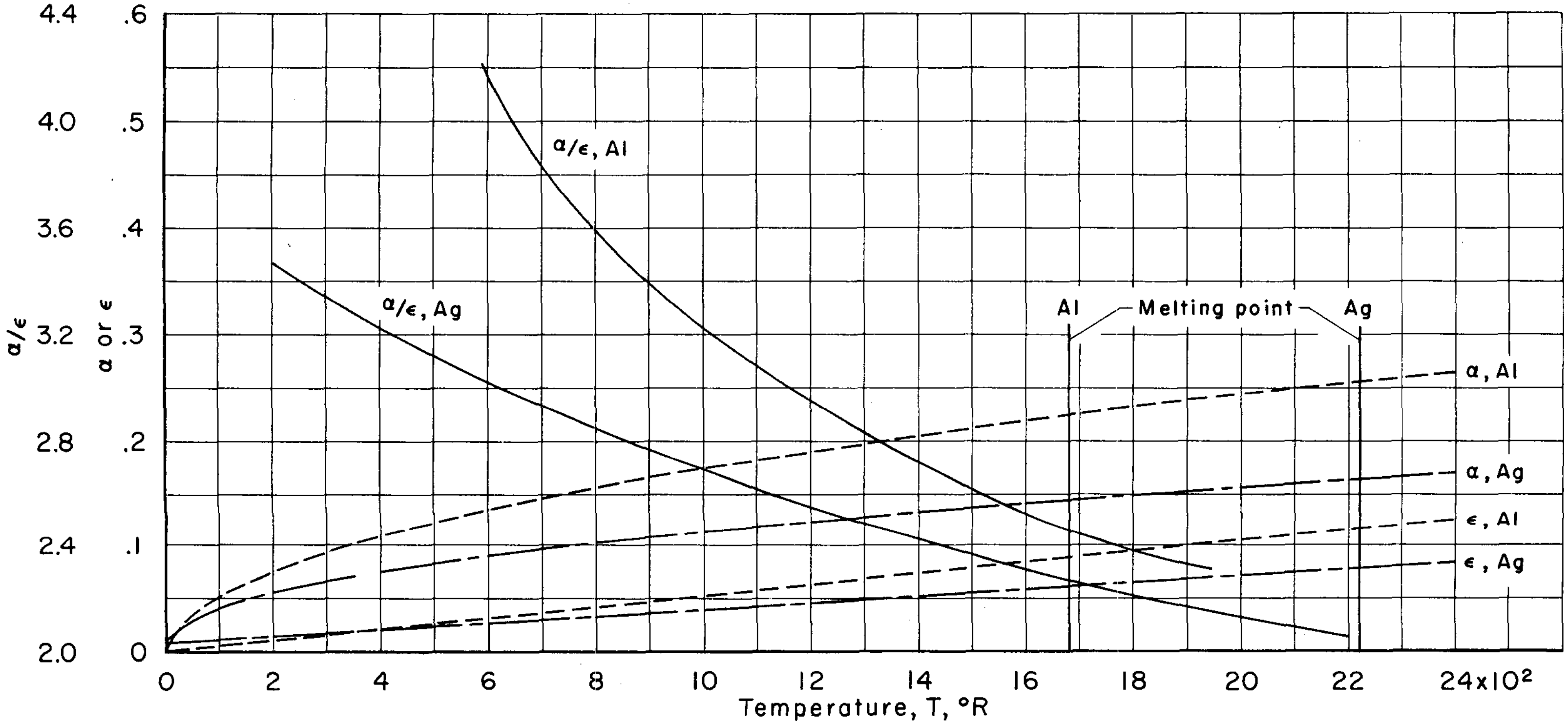

Figure 1.- Variations with temperature of emissivity and absorptivity and of their ratio for two metals.

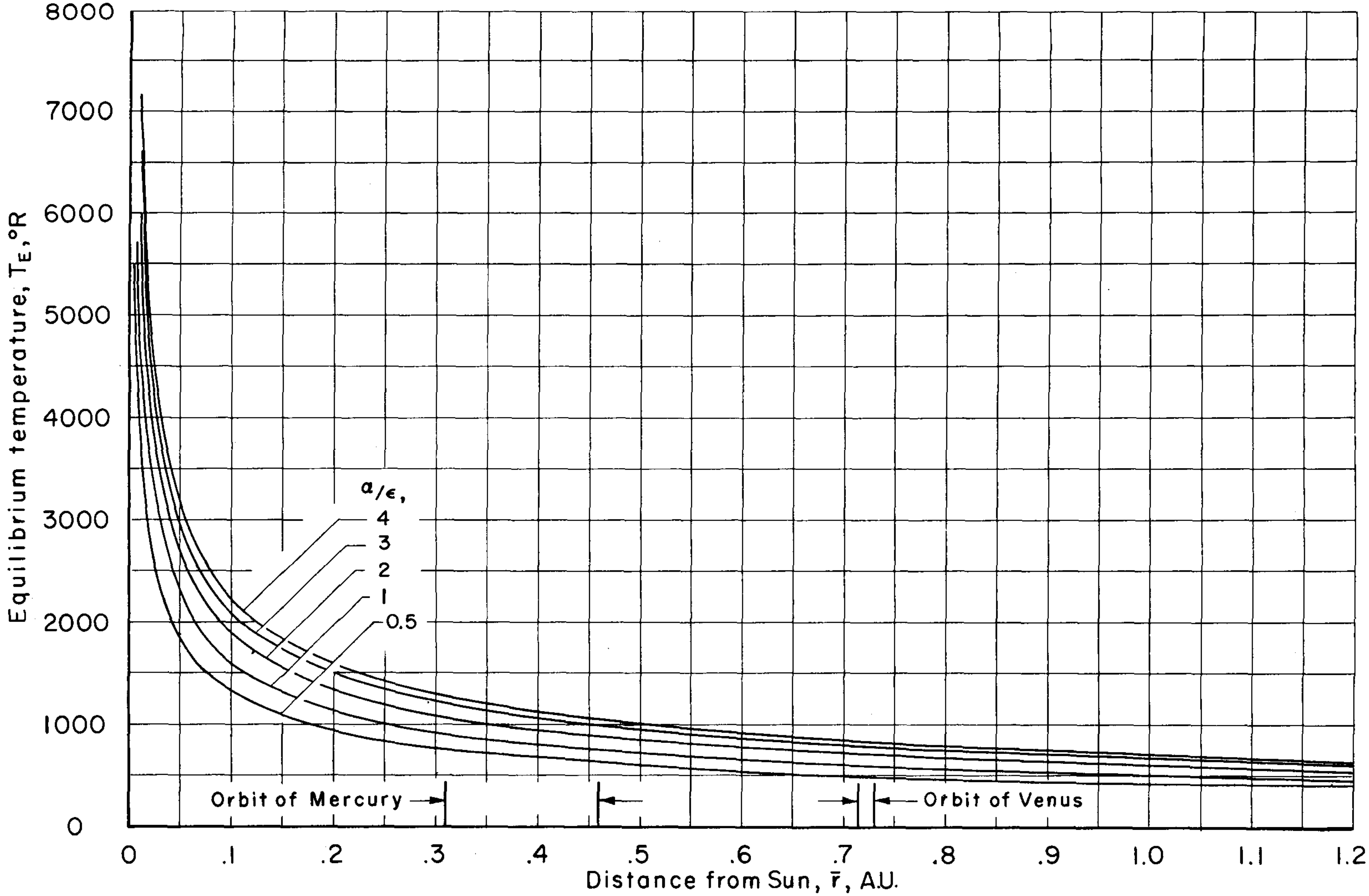

Figure 2.- Variation of equilibrium temperature with distance from the Sun in case of a sphere having uniform temperature.

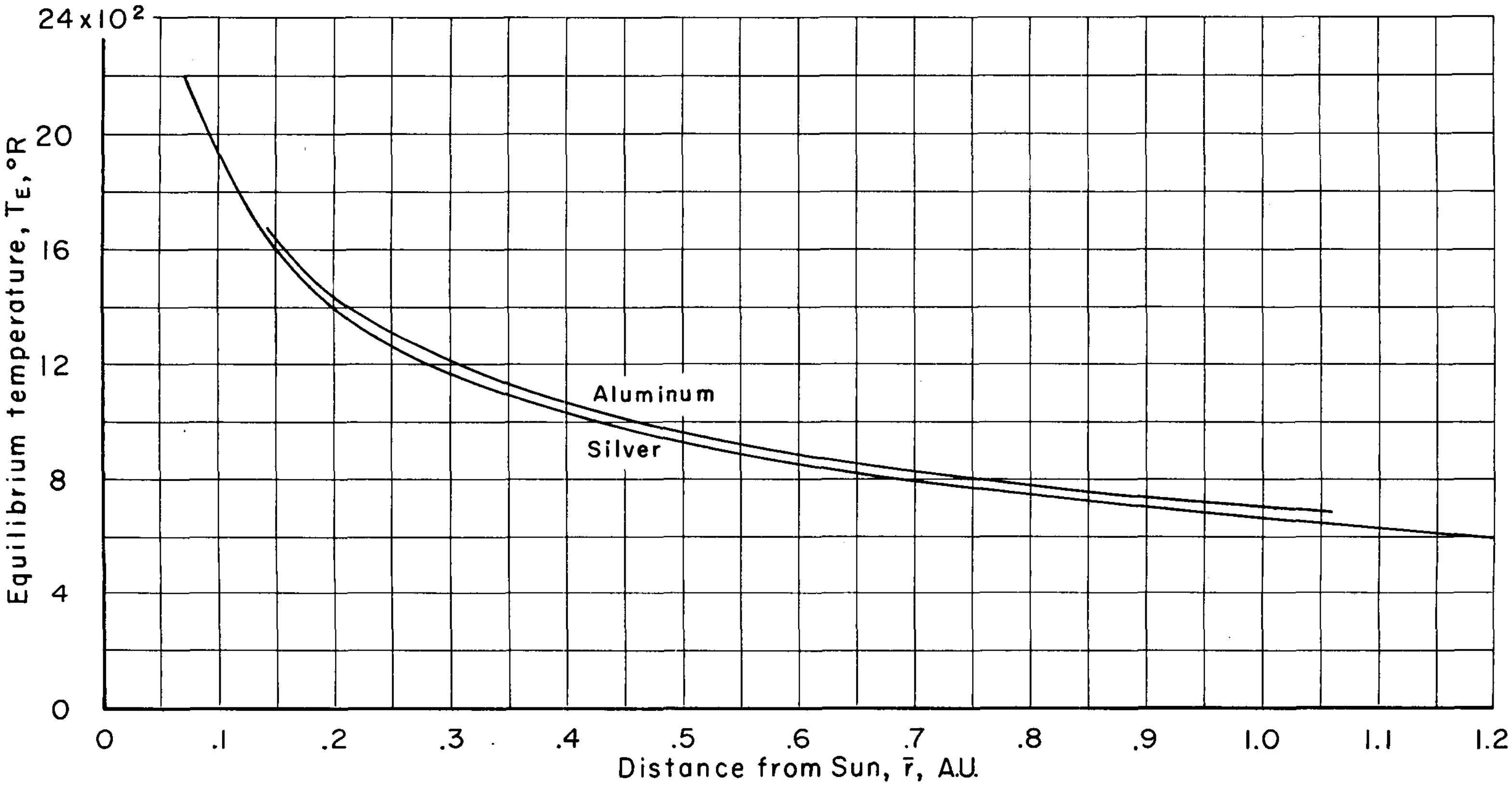

Figure 3.- Variation of equilibrium temperature with distance from Sun in case of aluminum or silver sphere having uniform temperature.

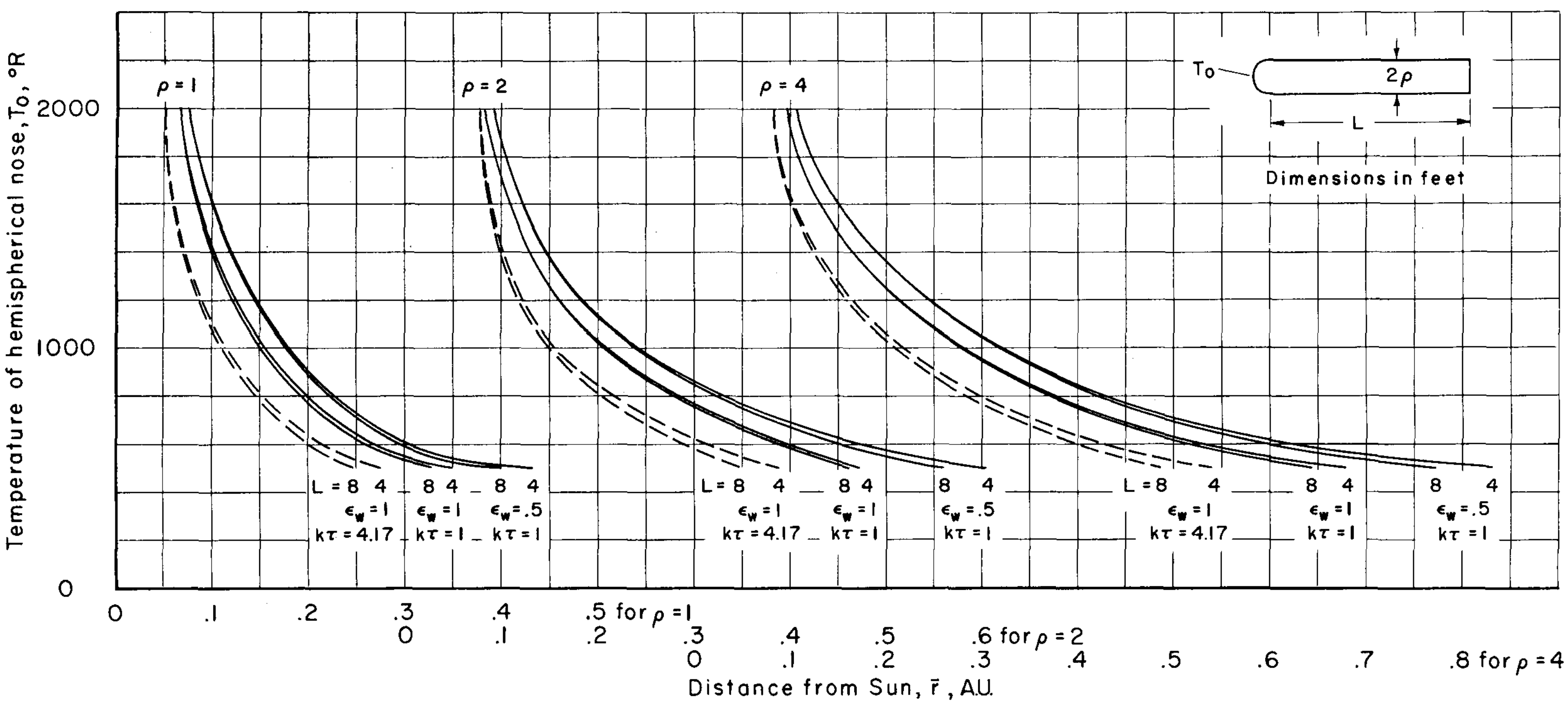

Figure 4.- Effects of several thermal and geometric factors upon the variation with distance from the Sun of temperature of hemispherical nose of probe.

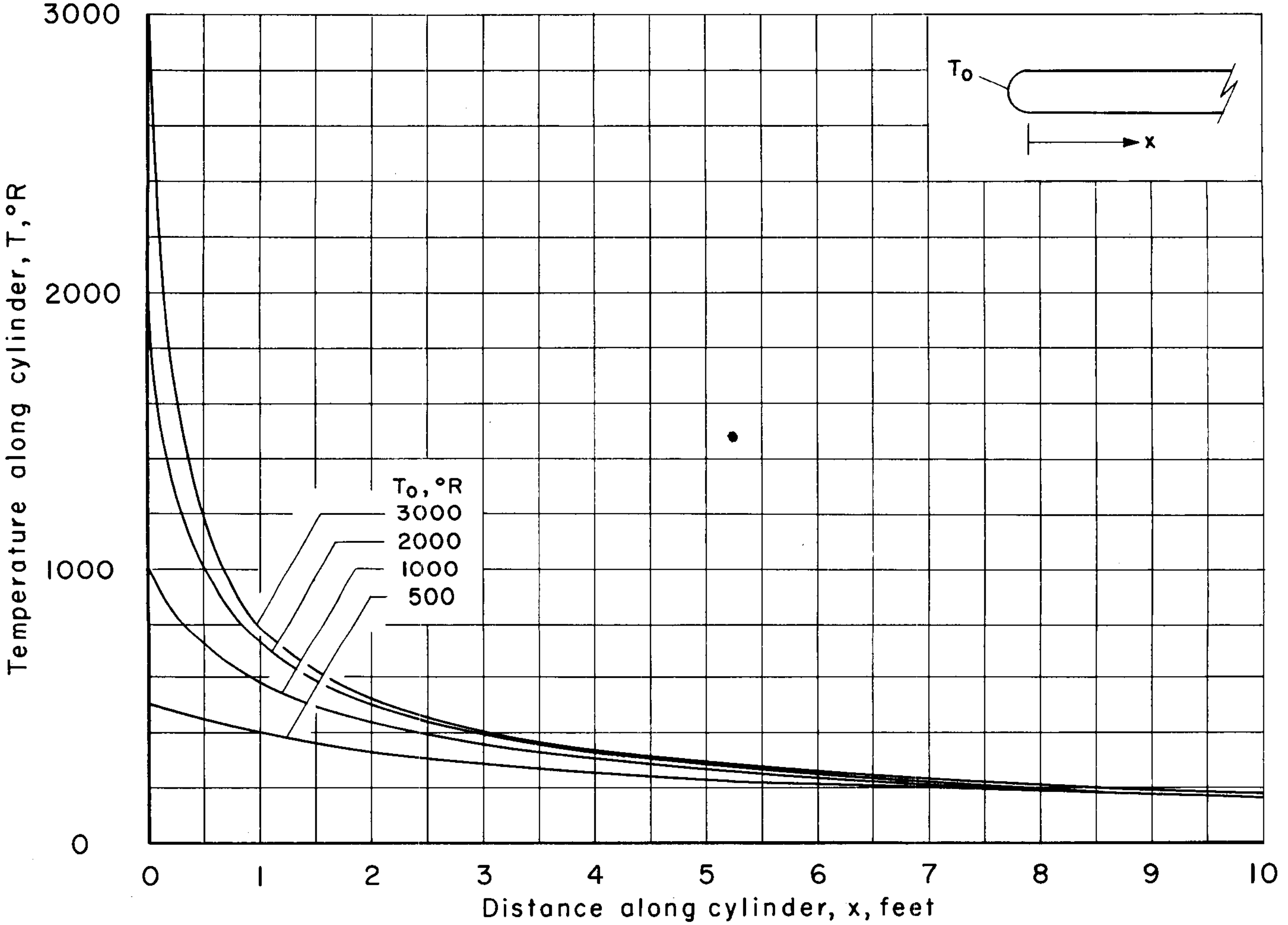

(a) $k\tau = 1.0$, $\epsilon_W = 1.0$.

Figure 5.- Variation of temperature along cylindrical section of probe for various assumed values of temperature of hemispherical nose.

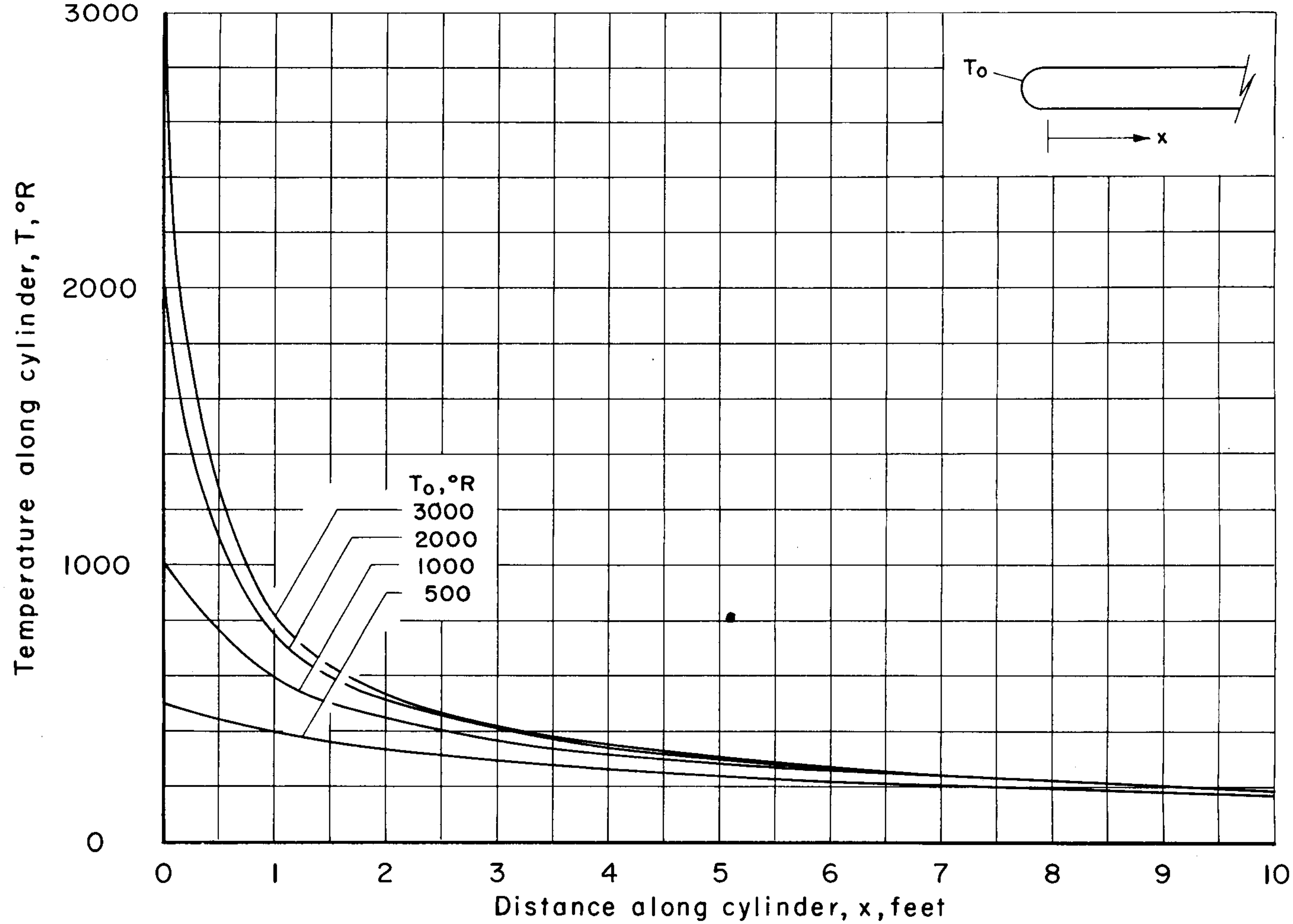

(b) $k\tau = 1.0$, $\epsilon_W = 0.9$.

Figure 5.- Continued.

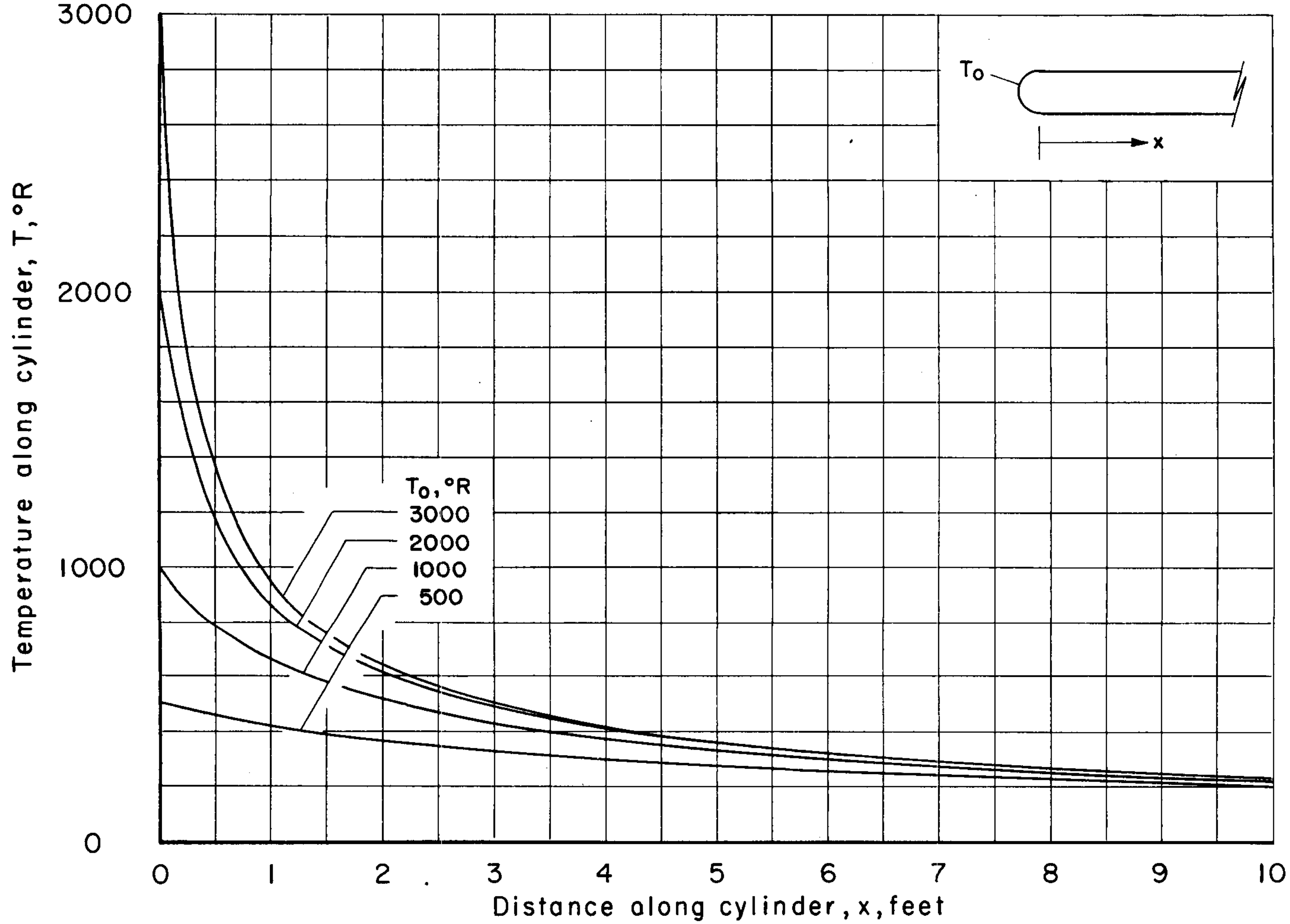

(c) $k\tau = 1.0$, $\epsilon_w = 0.5$.

Figure 5.- Continued.

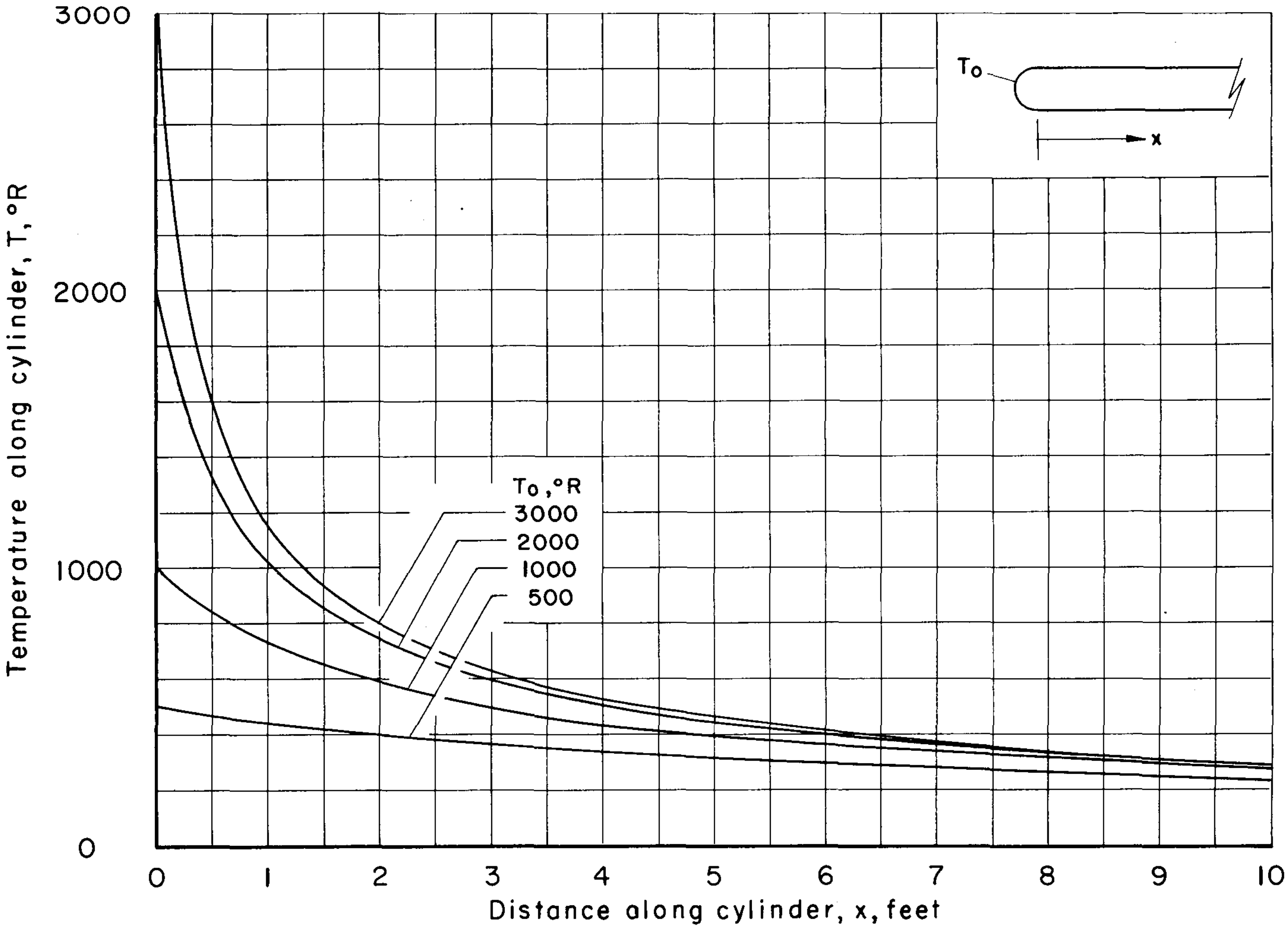

(d) $k\tau = 4.17$, $\epsilon_w = 1.0$.

Figure 5.- Continued.

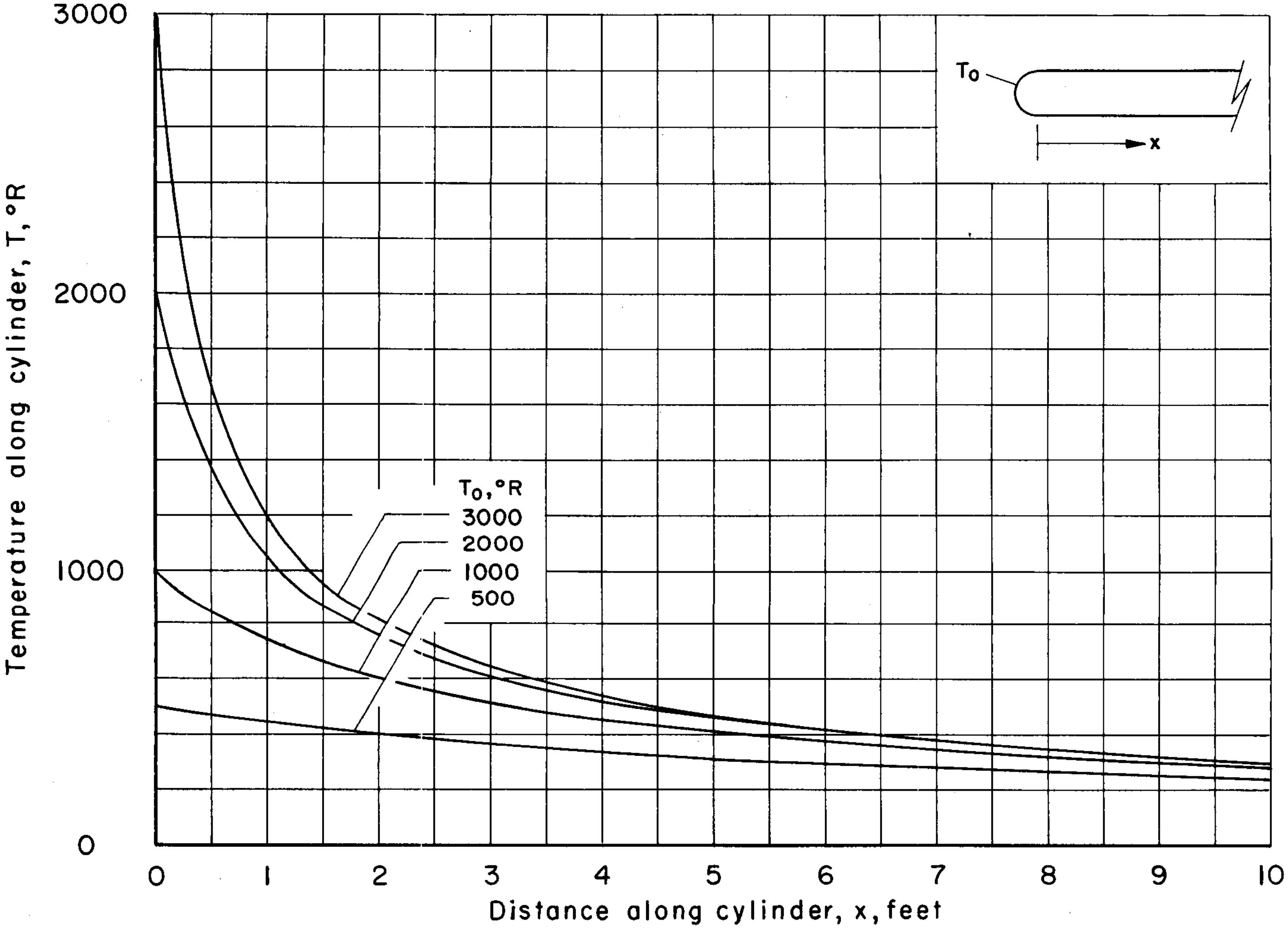

(e) $k\tau = 4.17$, $\epsilon_W = 0.9$.

Figure 5.- Continued.

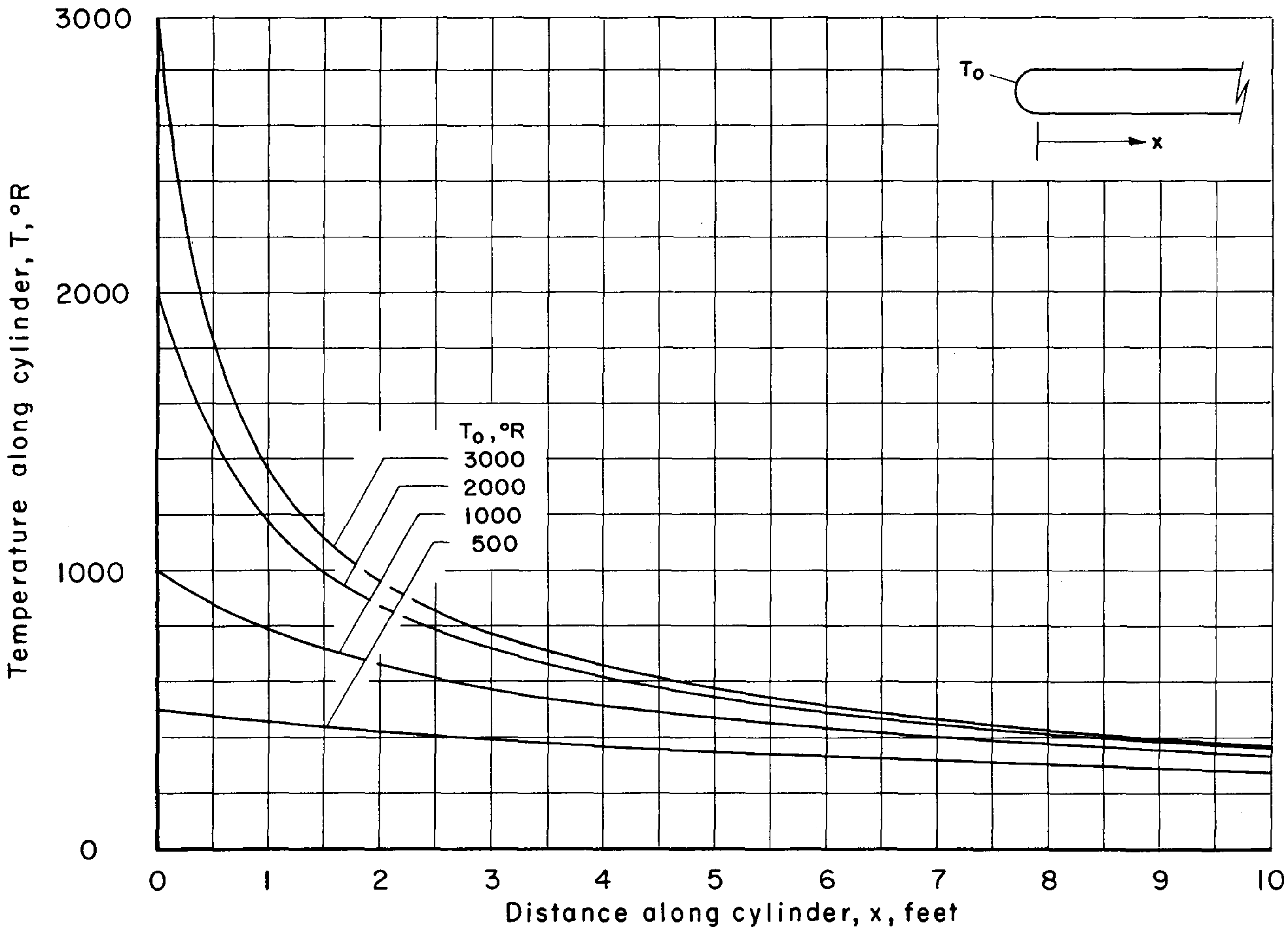

(f) $k\tau = 4.17$, $\epsilon_W = 0.5$.

Figure 5.- Concluded.

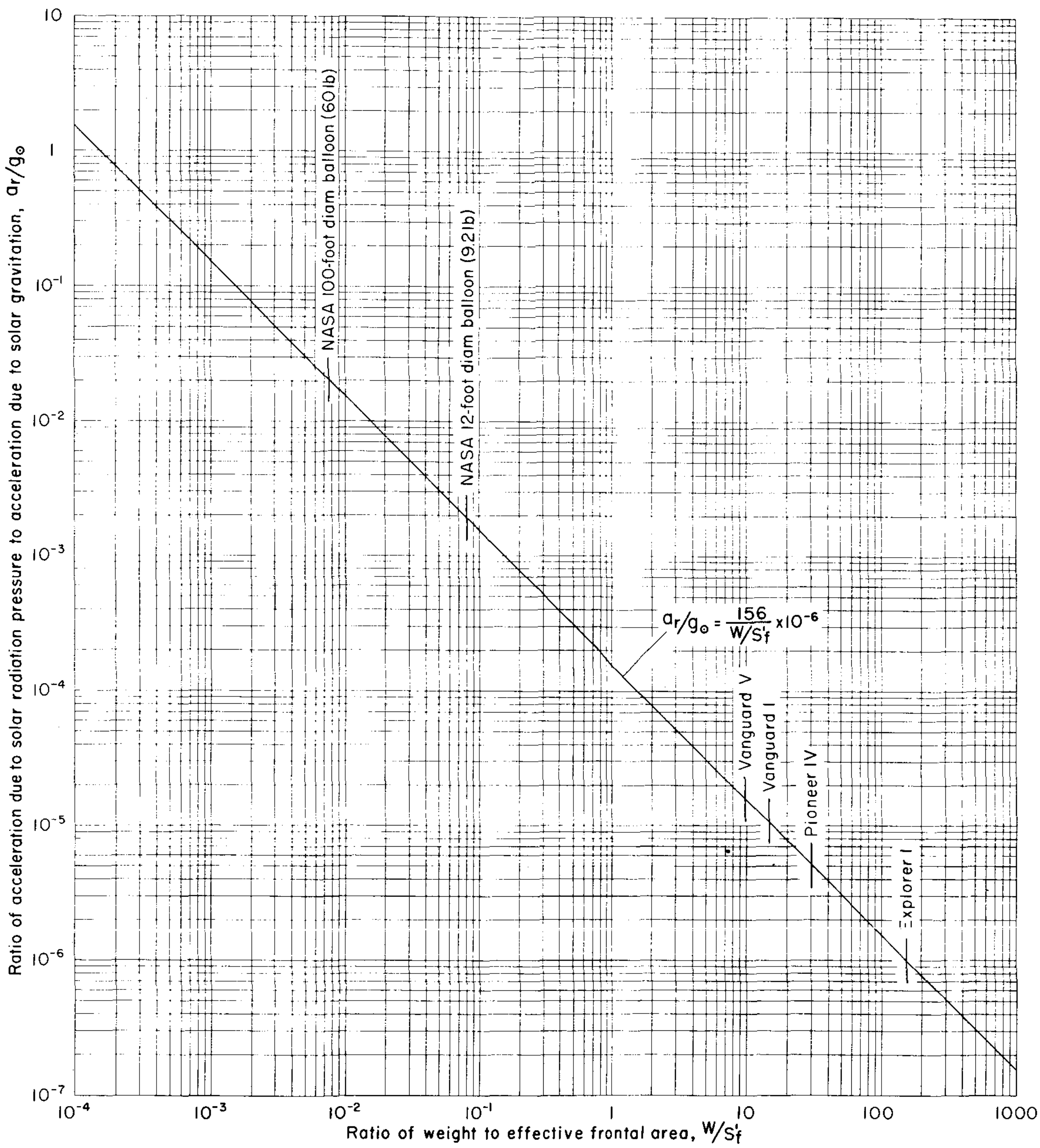

Figure 6.- Effects of radiation pressure.

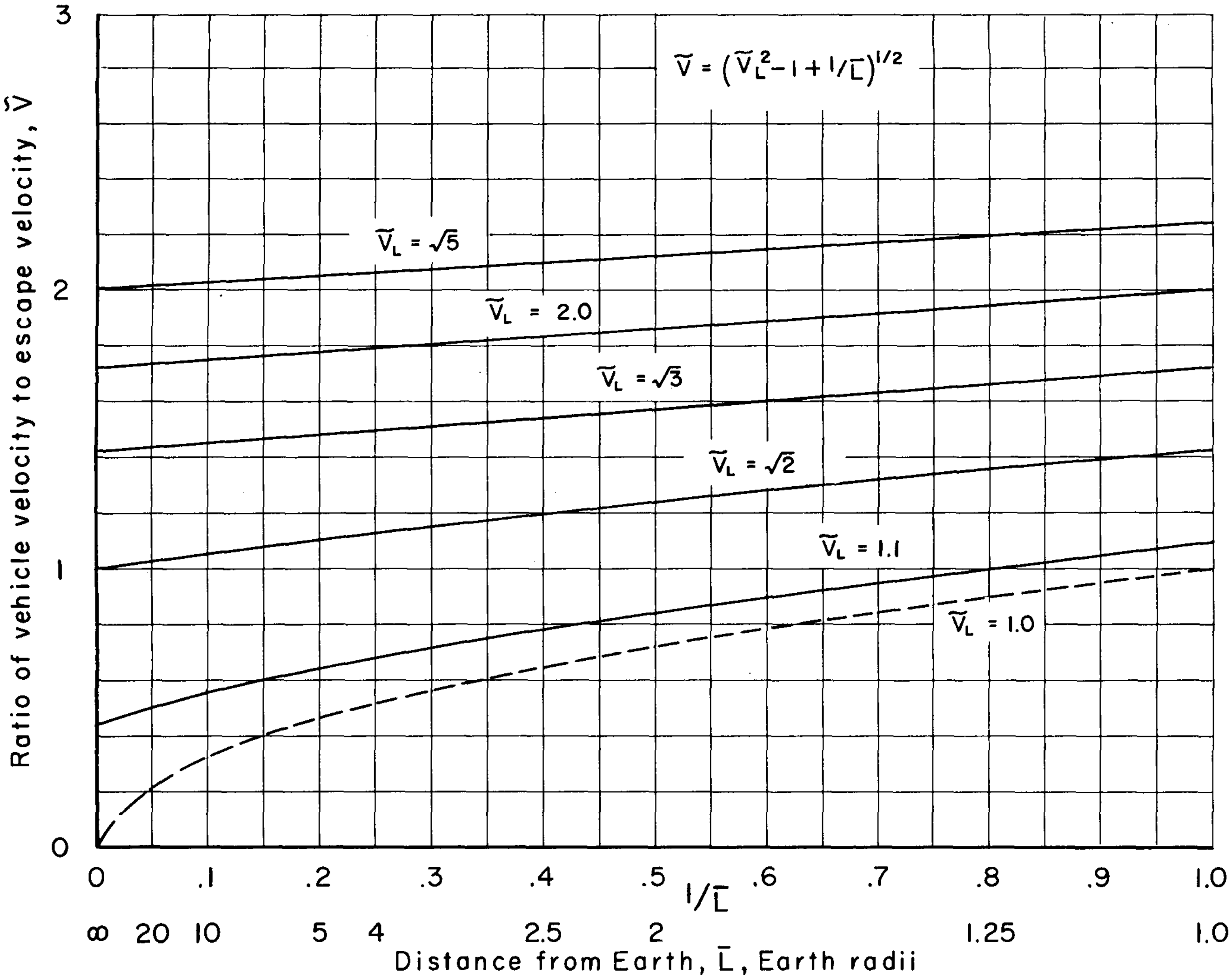

Figure 7.- Variation of velocity with distance from Earth for a body launched from surface of Earth with various burnout velocities.

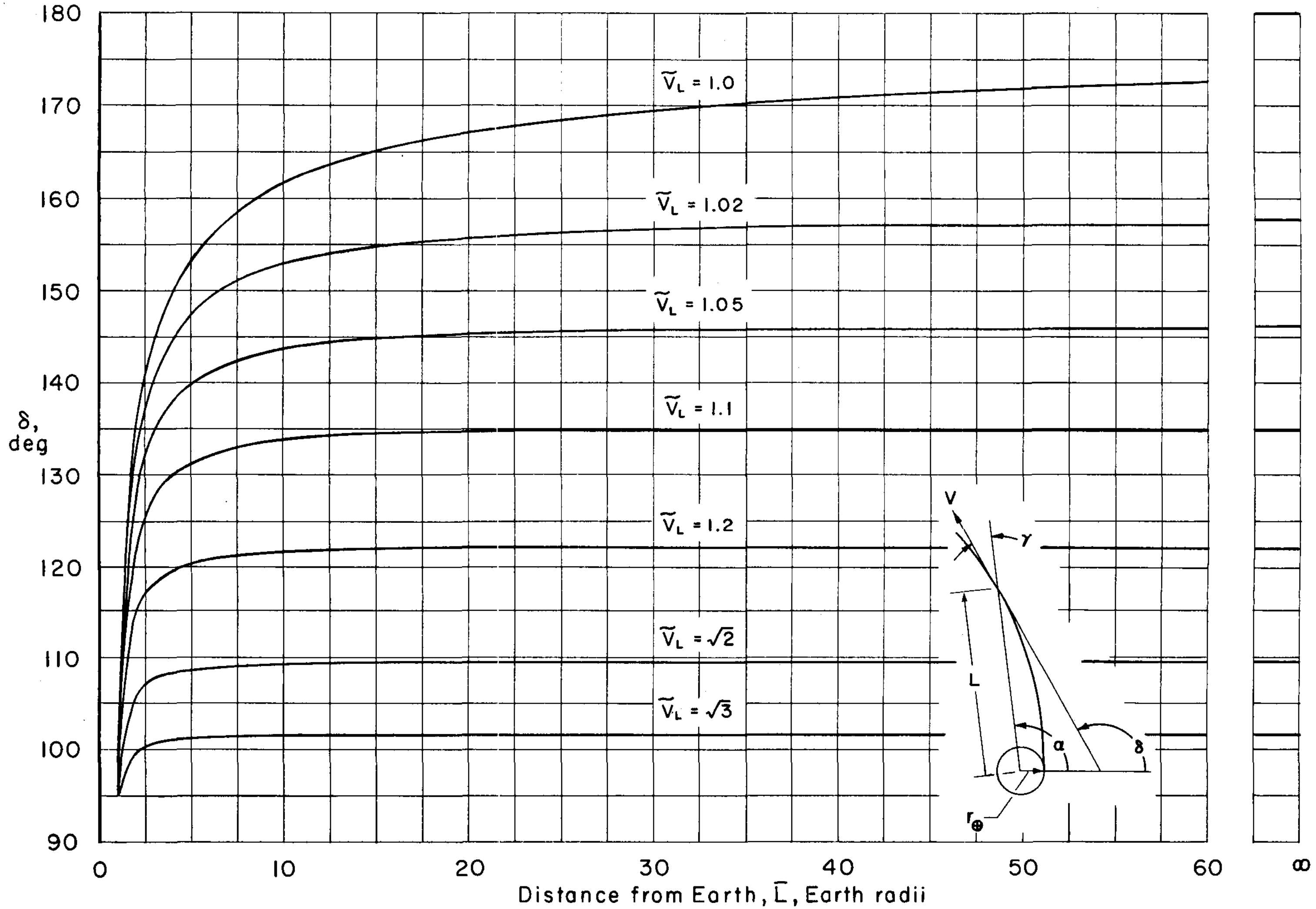

Figure 8.- Variation of direction of velocity with distance from Earth for a body launched from surface of Earth with various burnout velcocities.

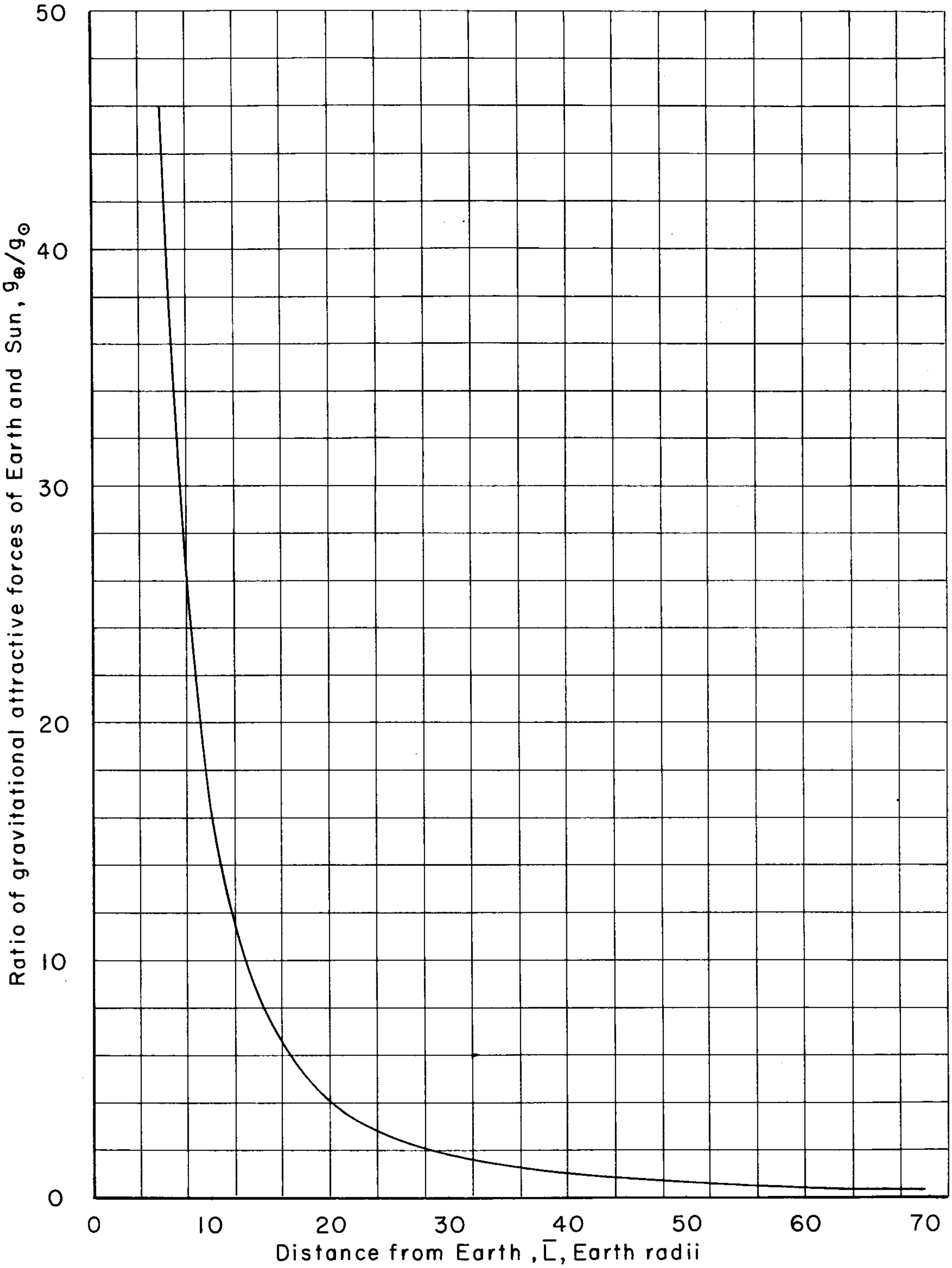

Figure 9.- Variation of the ratio of the gravitational accelerations of Earth and Sun with distance from the Earth along orbit of Earth.

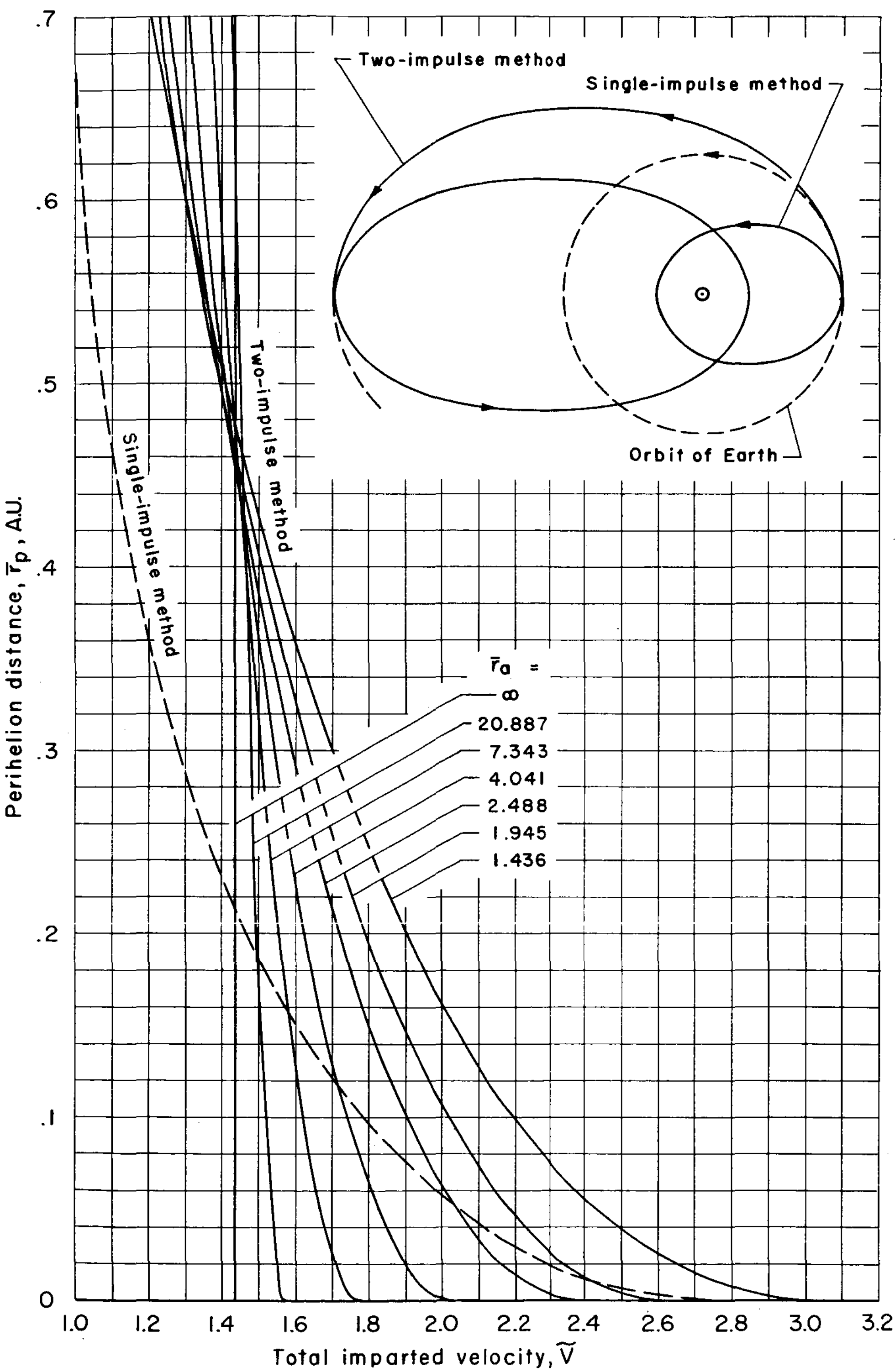

Figure 10.- Variation of perihelion distance obtained with total imparted velocity for both single-impulse and two-impulse methods.

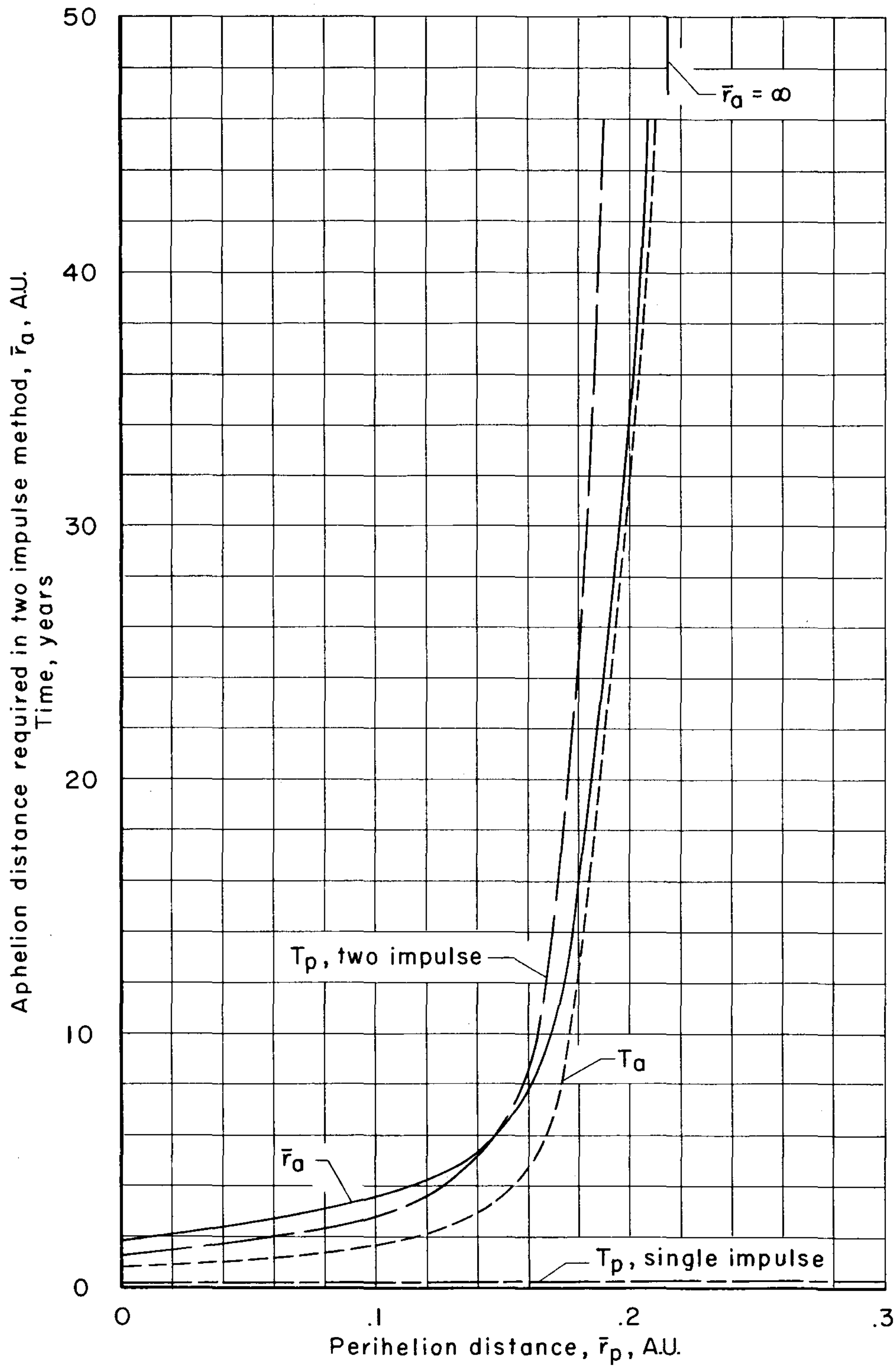

Figure 11.- Distance to aphelion and times required in two-impulse method to achieve same perihelion distance with same velocity requirements as in single-impulse method.

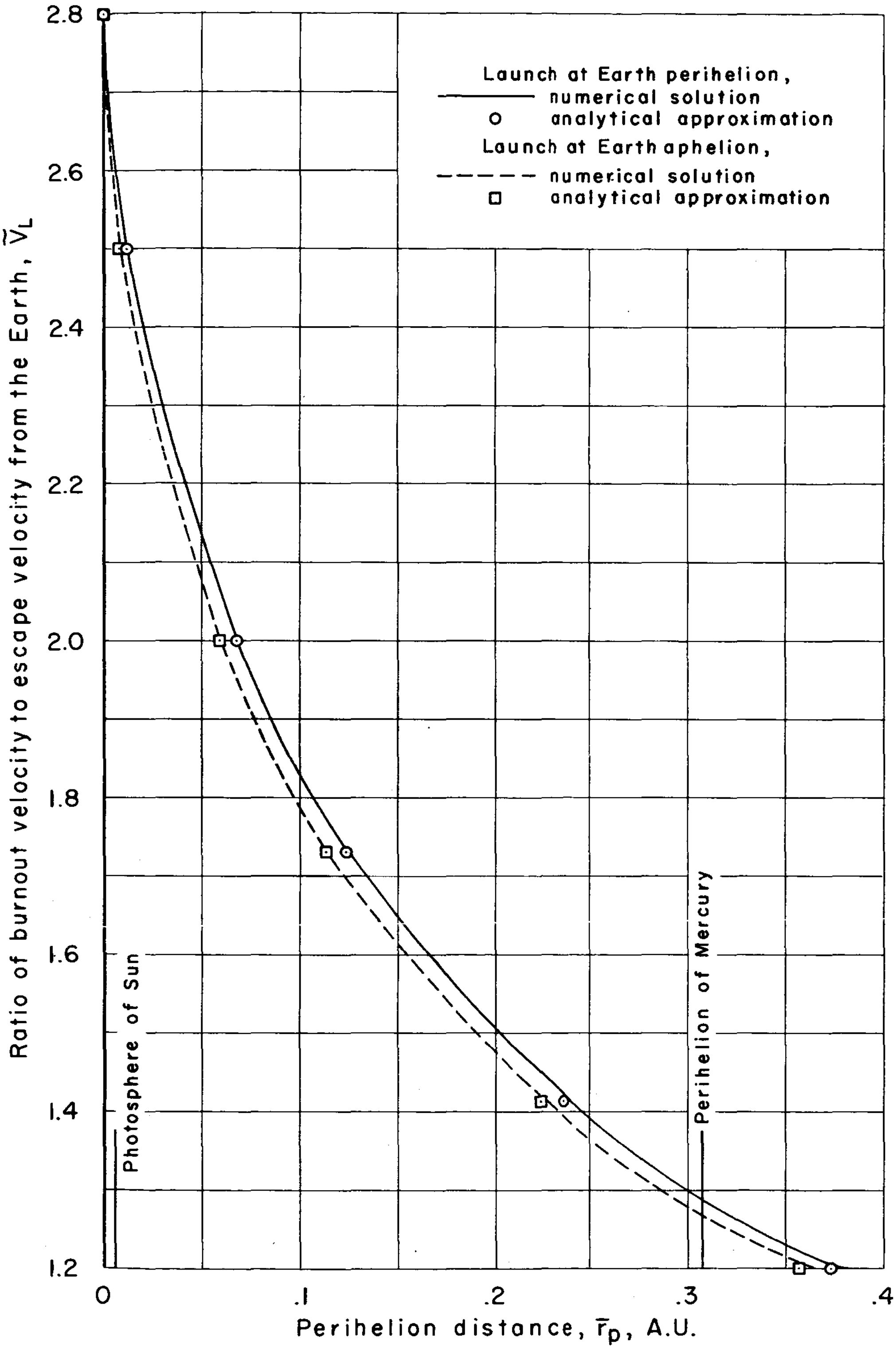

Figure 12.- Burnout velocities required for given perihelion distances of solar-probe orbits.

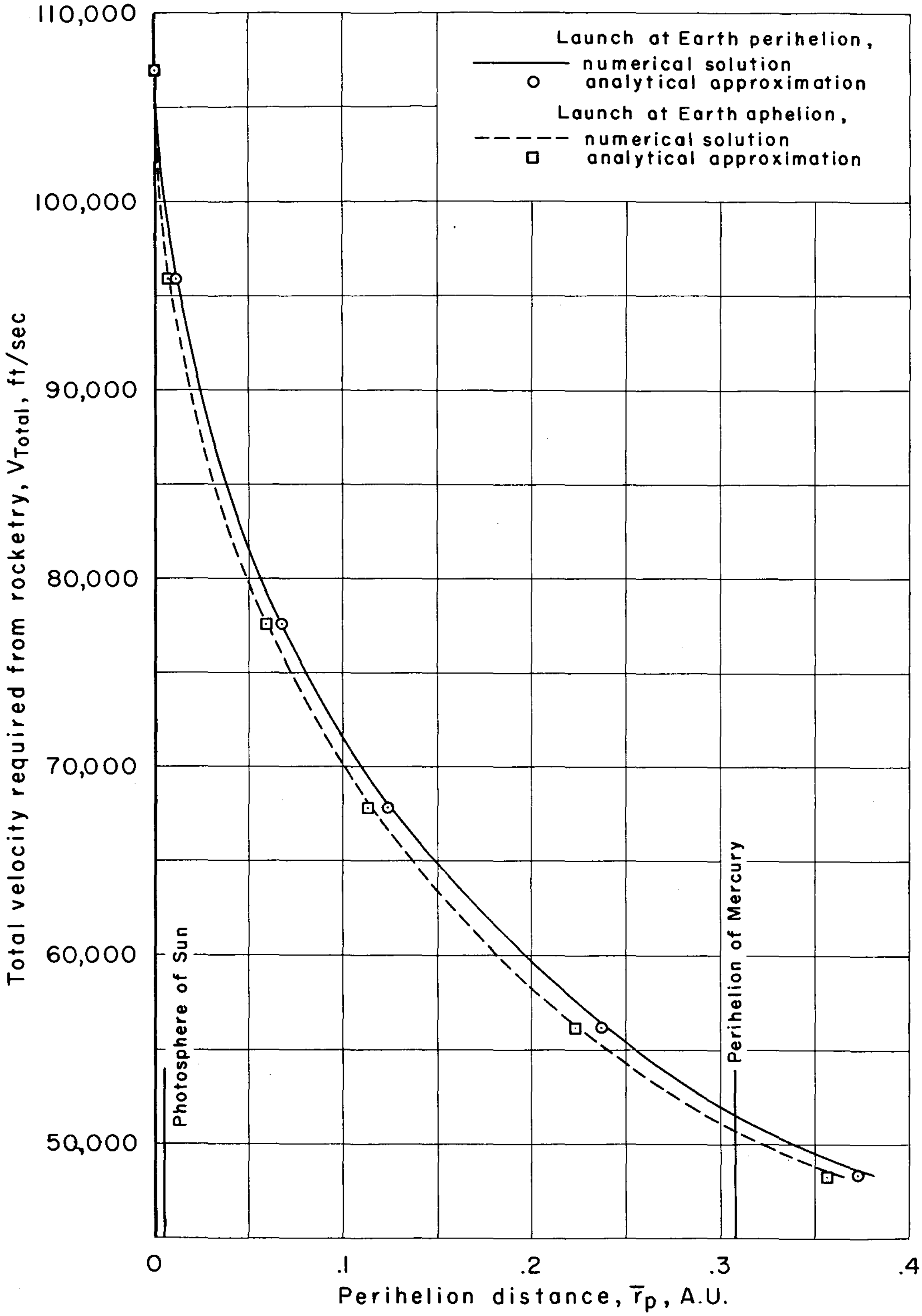

Figure 13.- Total velocities required from propulsion to achieve given perihelion distances of solar-probe orbits.

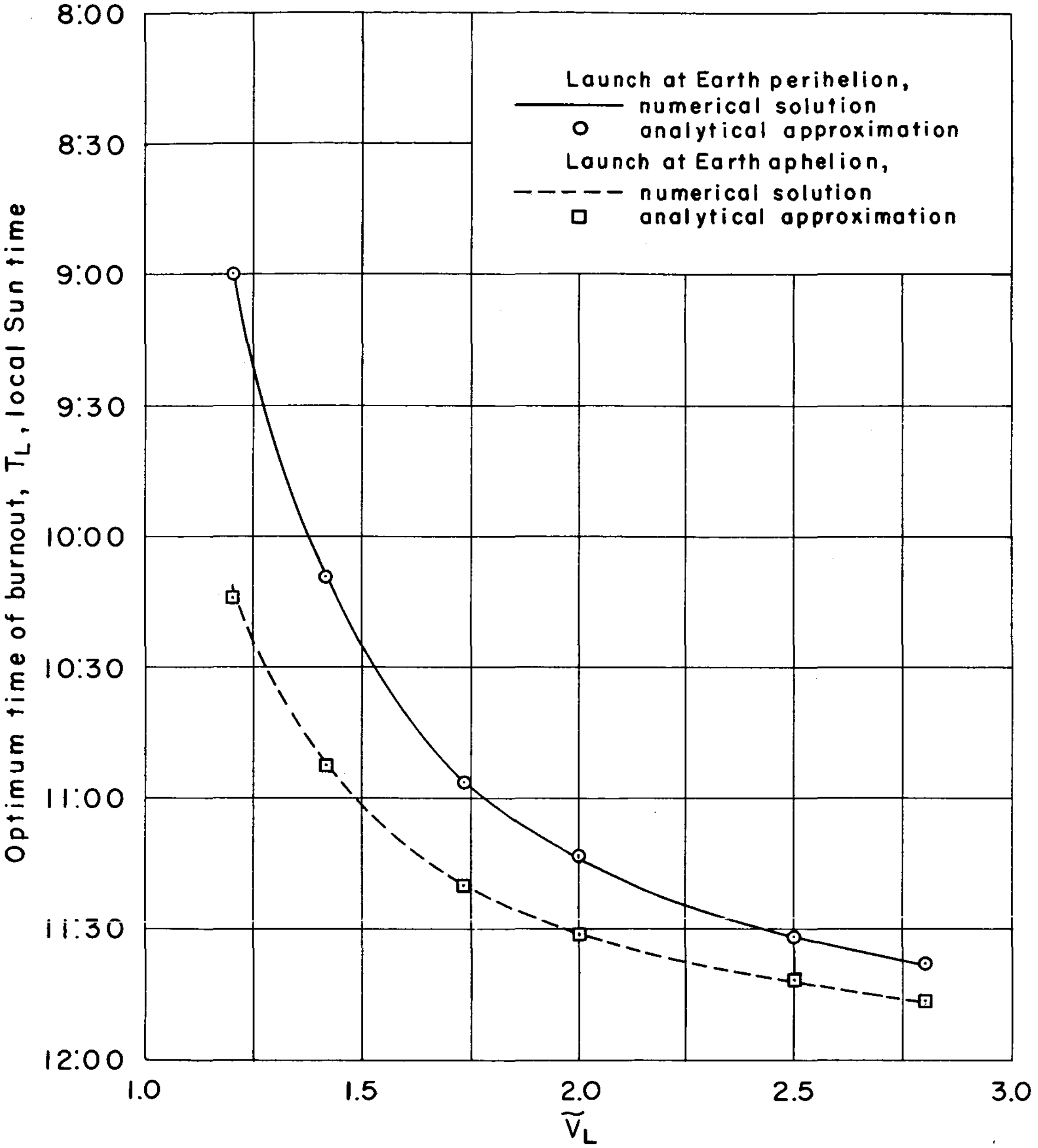

Figure 14.- Time at which burnout should occur to obtain least perihelion distance for given burnout velocity as a function of burnout velocity.

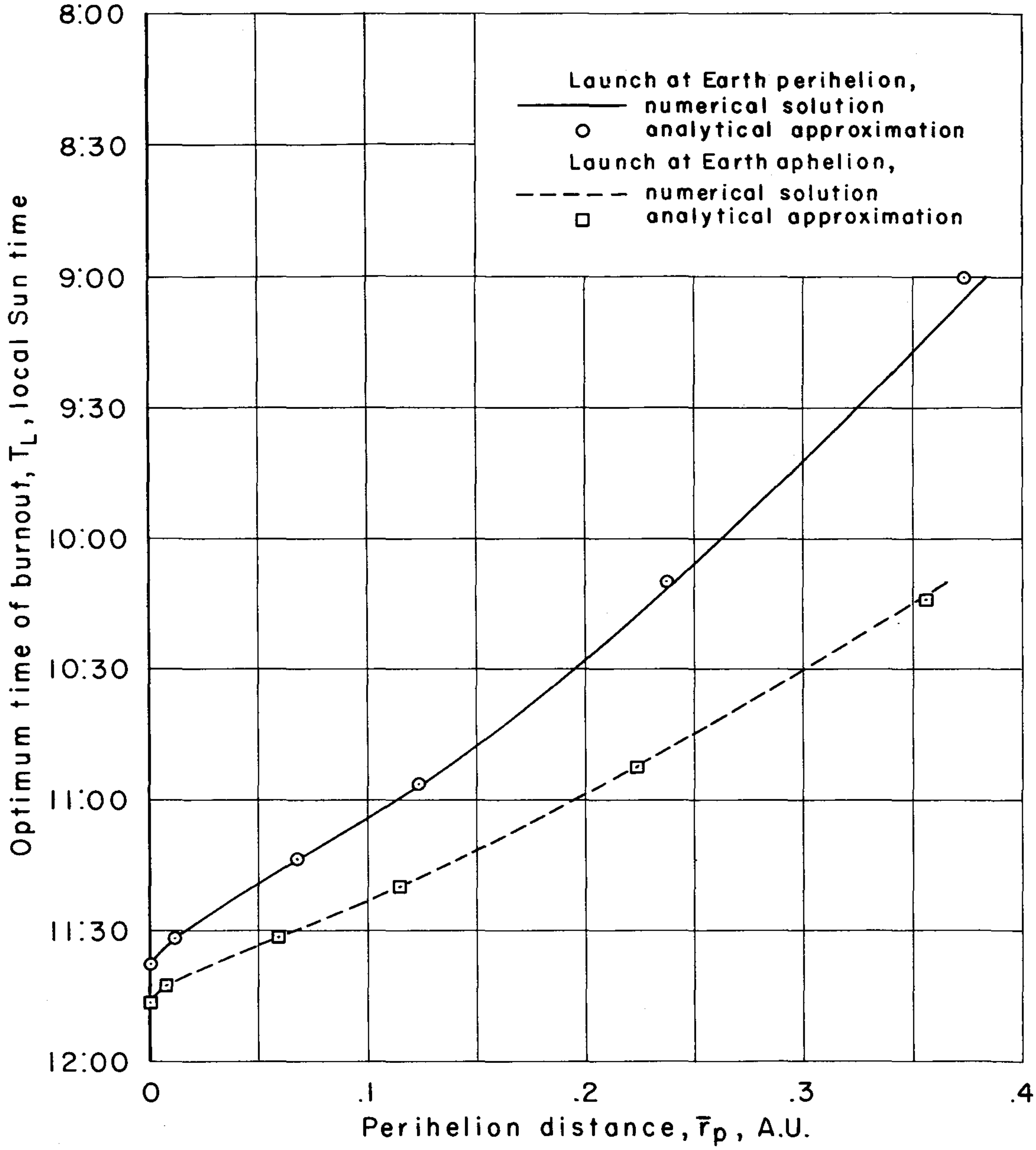

Figure 15.- Time at which burnout should occur to obtain least perihelion distance for given burnout velocity as a function of perihelion distance.

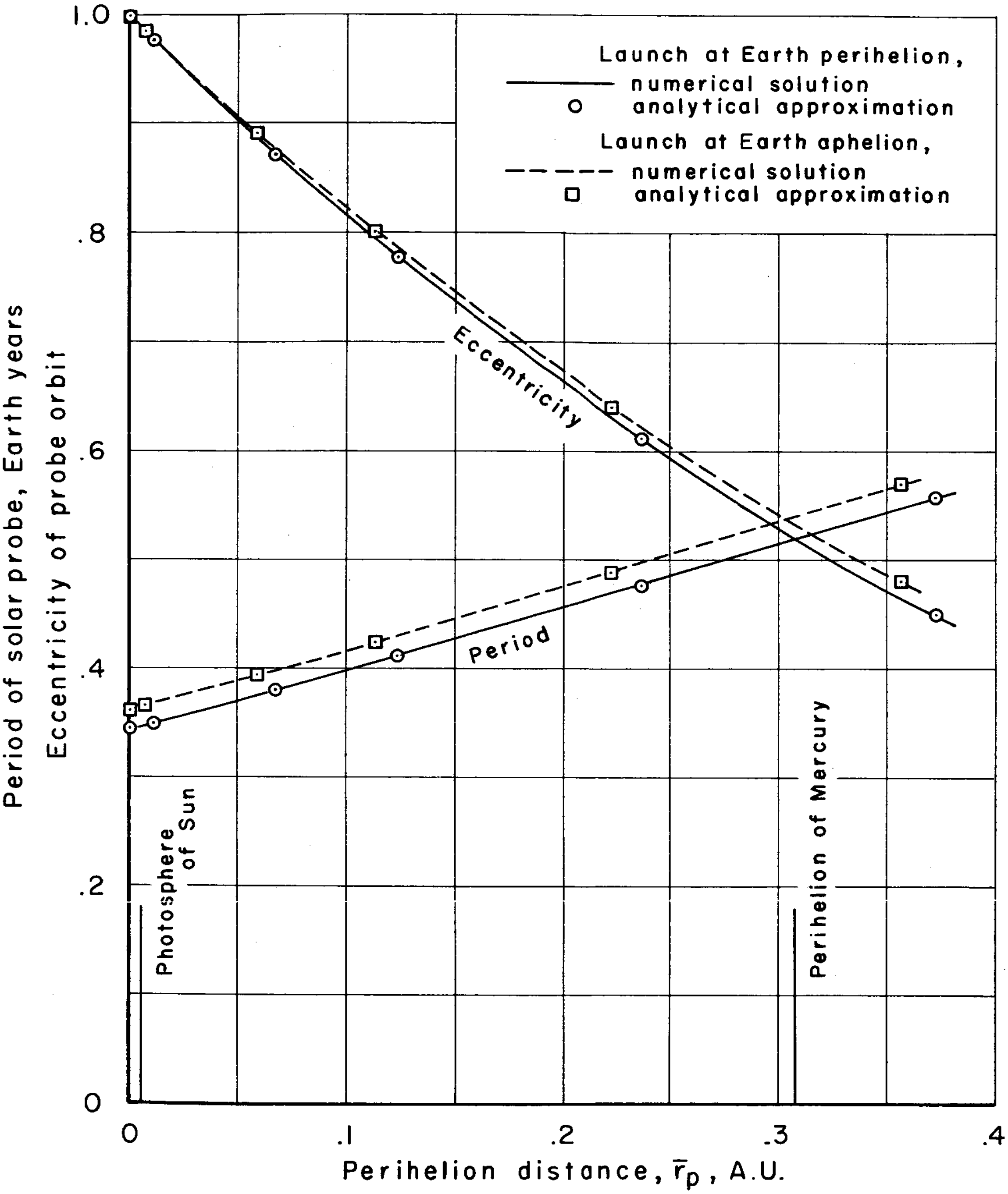

Figure 16.- Periods and eccentricities of solar-probe orbits having various perihelion distances.

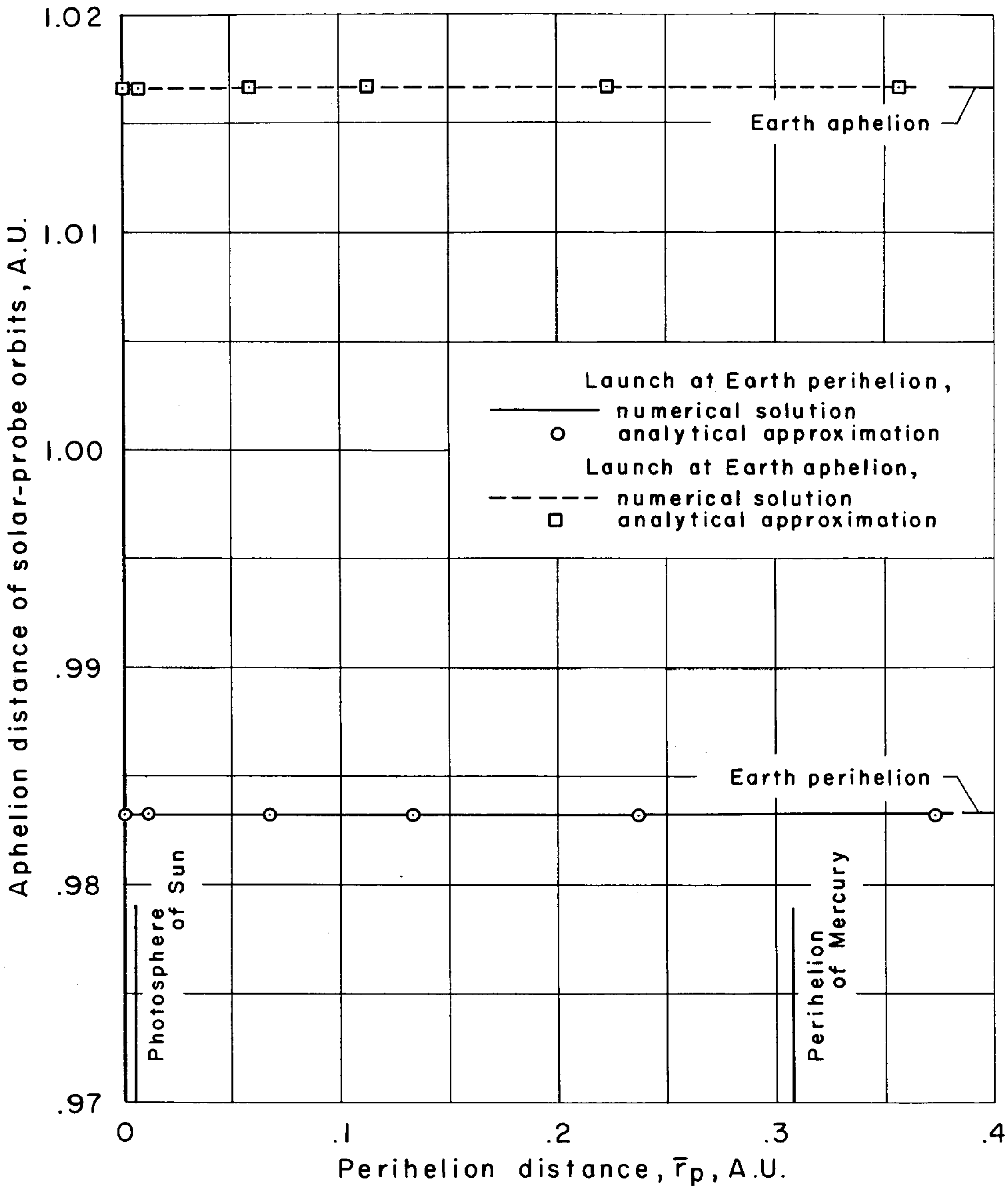

Figure 17.- Aphelion distances corresponding to perihelion distances of solar-probe orbits.

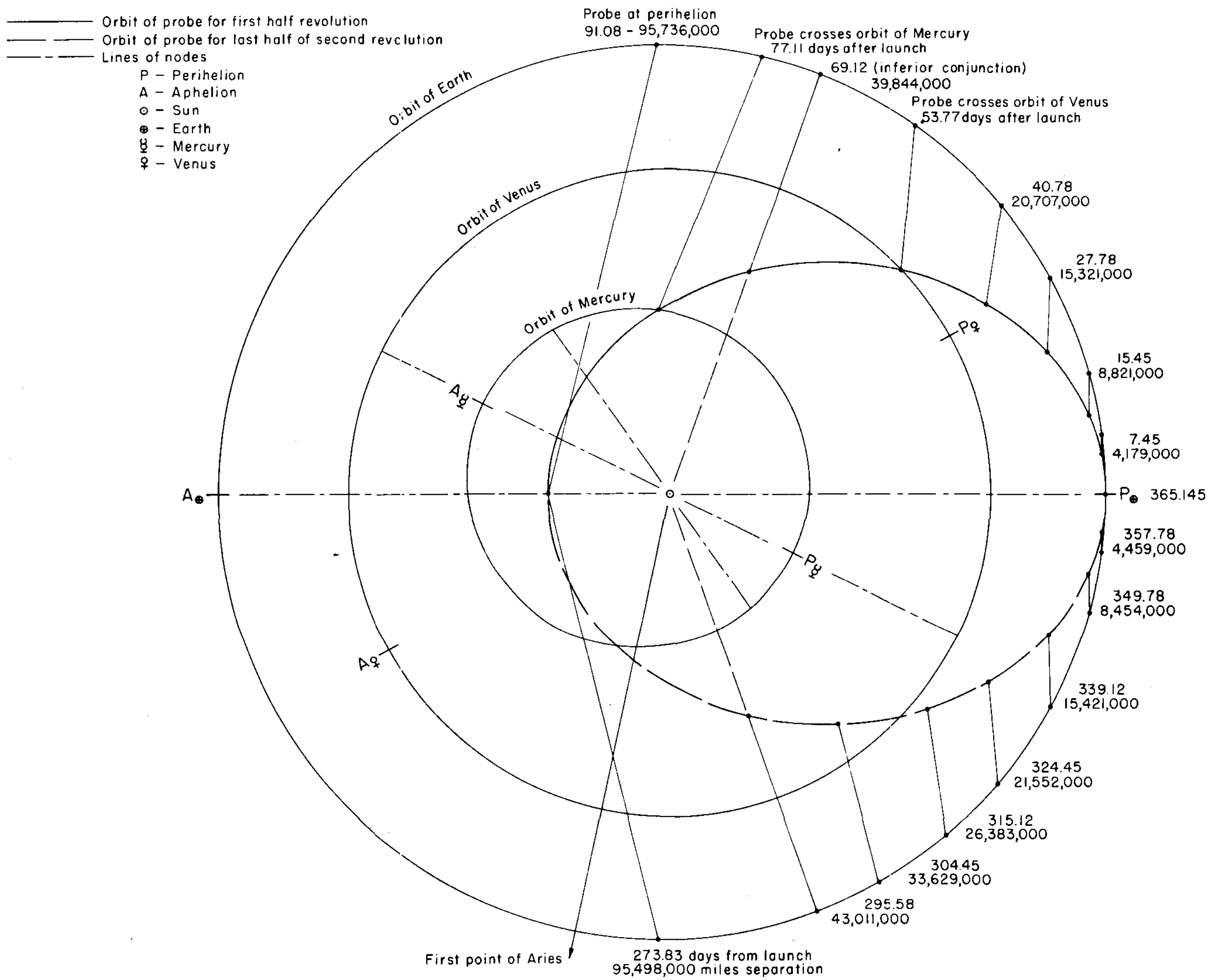

Figure 18.- Trajectory of probe which reaches its aphelion almost simultaneously with an inferior conjunction with respect to Earth and Sun.

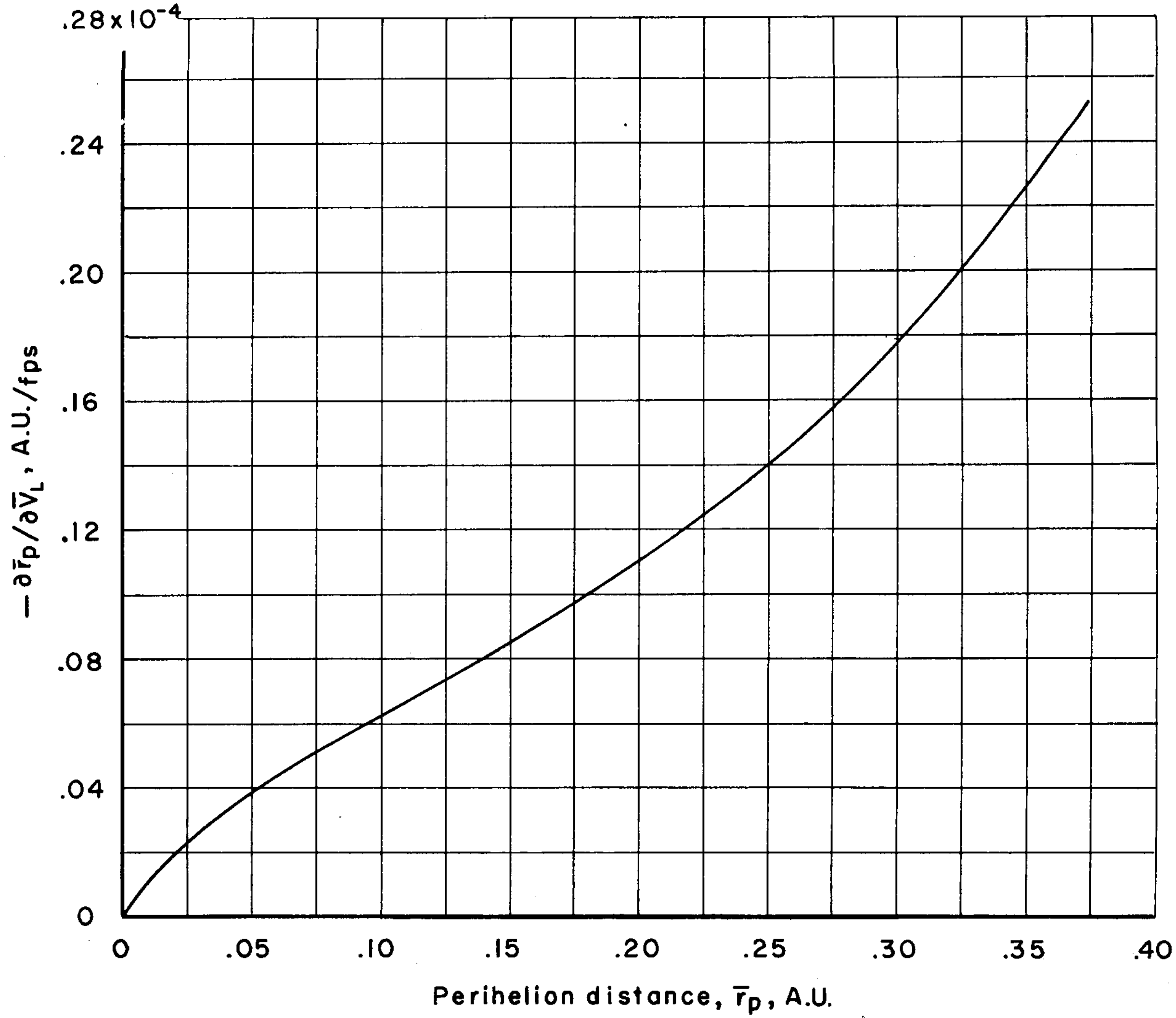

Figure 19.- Variation of the effect of errors in burnout velocity upon perihelion distance obtained, with perihelion distance.

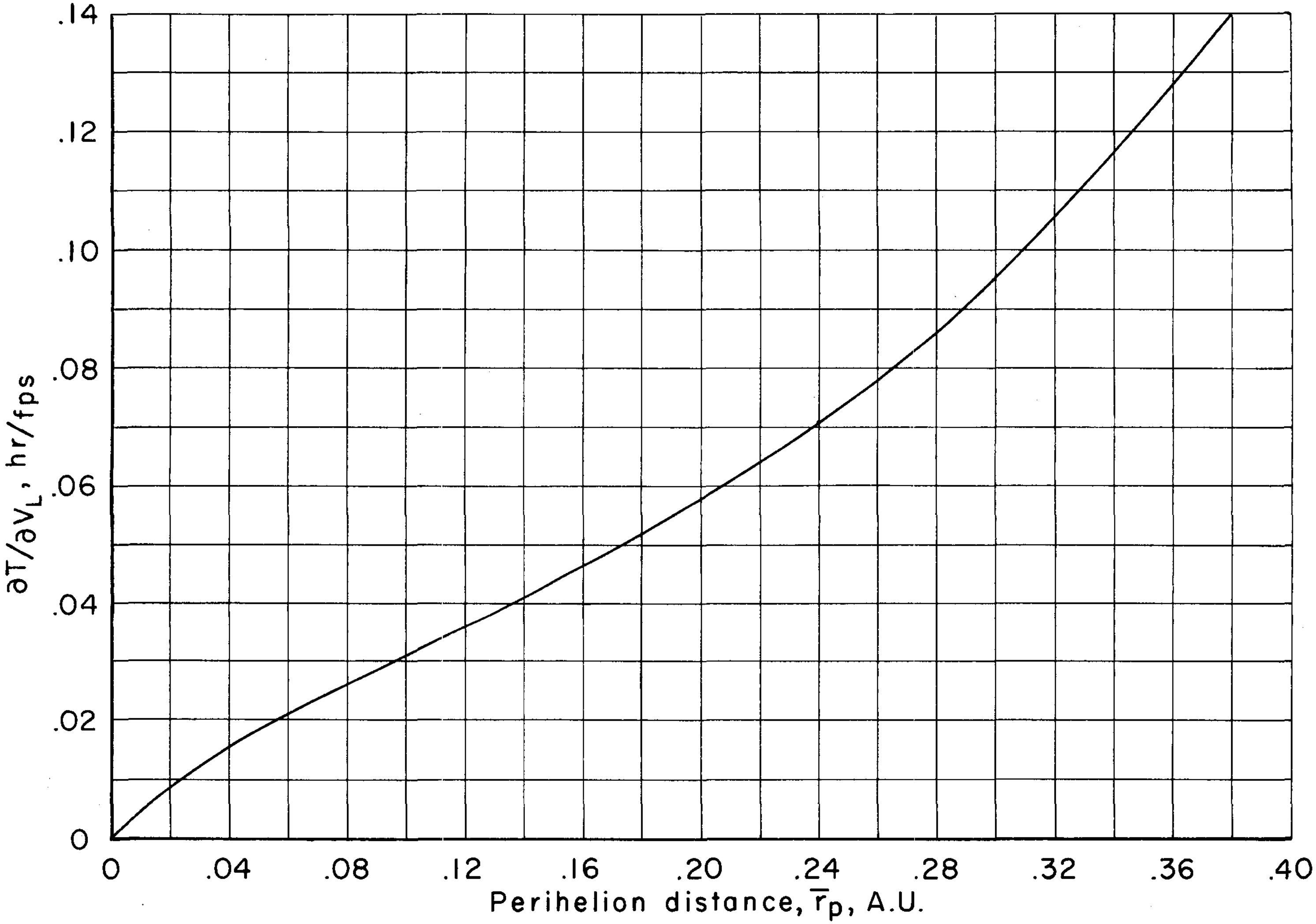

Figure 20.- Effect of error in burnout velocity upon period of solar-probe orbit of given perihelion distance.

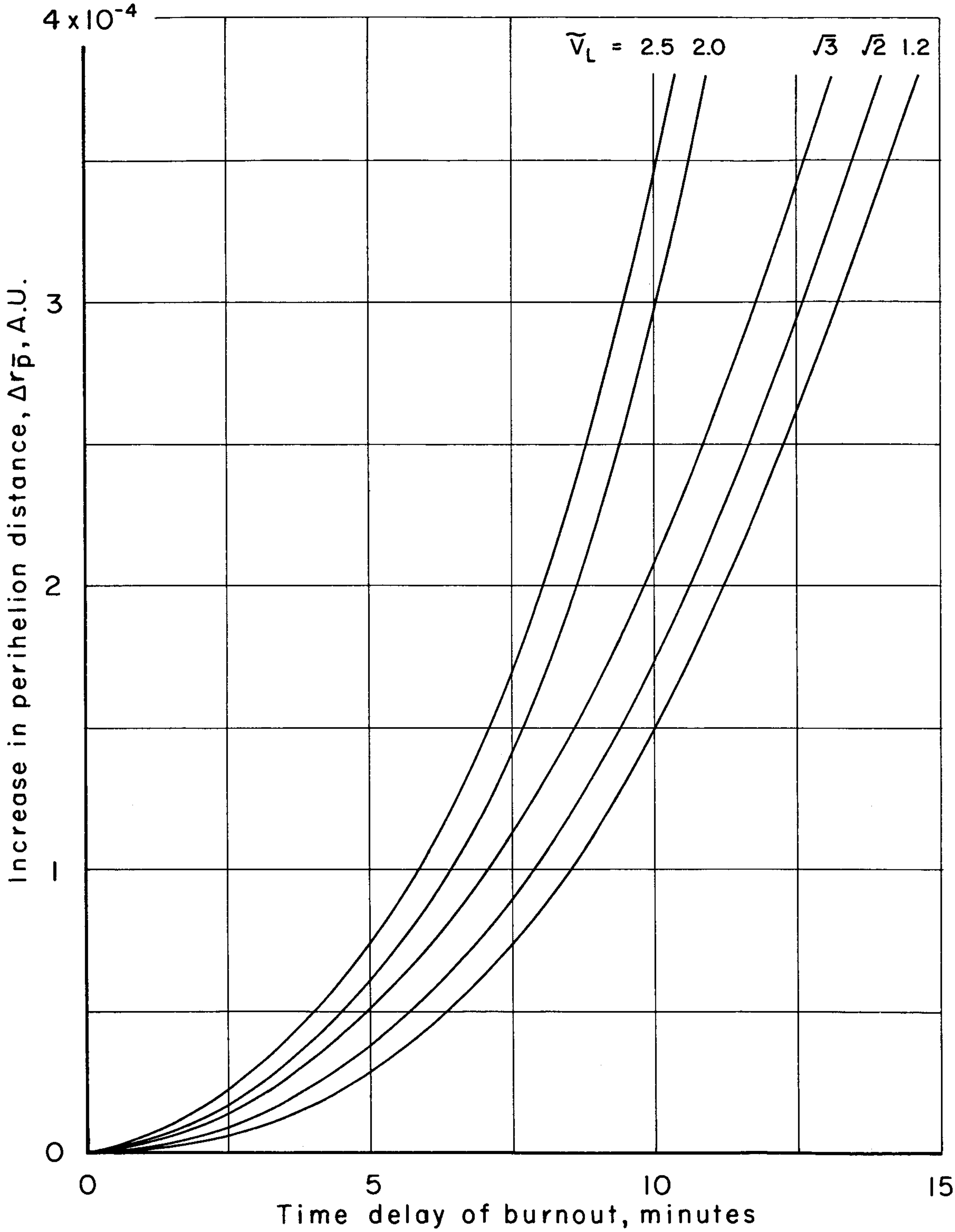

Figure 21.- Effects of delay in achieving burnout conditions upon perihelion distance obtained.